

Review

# A Review on Biochar as an Adsorbent for Pb(II) Removal from Water

Pushpita Kumkum and Sandeep Kumar \*

Department of Civil and Environmental Engineering, Old Dominion University, Norfolk, VA 23529, USA;  
pkumk001@odu.edu

\* Correspondence: skumar@odu.edu

**Abstract:** Heavy metal contamination in drinking water is a growing concern due to its severe health effects on humans. Among the many metals, lead (Pb), which is a toxic and harmful element, has the most widespread global distribution. Pb pollution is a major problem of water pollution in developing countries and nations. The most common sources of lead in drinking water are lead pipes, faucets, and plumbing fixtures. Adsorption is the most efficient method for metal removal, and activated carbon has been used widely in many applications as an effective adsorbent, but its high production costs have created the necessity for a low-cost alternative adsorbent. Biochar can be a cost-effective substitute for activated carbon in lead adsorption because of its porous structure, irregular surface, high surface-to-volume ratio, and presence of oxygenated functional groups. Extensive research has explored the remarkable potential of biochar in adsorbing Pb from water and wastewater through batch and column studies. Despite its efficacy in Pb removal, several challenges hinder the real application of biochar as an adsorbent. These challenges include variability in the adsorption capacity due to the diverse range of biomass feedstocks, production processes, pH dependence, potential desorption, or a leaching of Pb from the biochar back into the solution; the regeneration and reutilization of spent biochar; and a lack of studies on scalability issues for its application as an adsorbent. This manuscript aims to review the last ten years of research, highlighting the opportunities and engineering challenges associated with using biochar for Pb removal from water. Biochar production and activation methods, kinetics, adsorption isotherms, mechanisms, regeneration, and adsorption capacities with process conditions are discussed. The objective is to provide a comprehensive resource that can guide future researchers and practitioners in addressing engineering challenges.



**Citation:** Kumkum, P.; Kumar, S. A Review on Biochar as an Adsorbent for Pb(II) Removal from Water.

*Biomass* **2024**, *4*, 243–272. <https://doi.org/10.3390/biomass4020012>

Academic Editor: Maurizio Volpe

Received: 21 January 2024

Revised: 7 March 2024

Accepted: 15 March 2024

Published: 2 April 2024



**Copyright:** © 2024 by the authors. Licensee MDPI, Basel, Switzerland. This article is an open access article distributed under the terms and conditions of the Creative Commons Attribution (CC BY) license (<https://creativecommons.org/licenses/by/4.0/>).

**Keywords:** biochar; heavy metals; lead; adsorption; pollutant removal; biomass; desorption; regeneration; scalability

## 1. Introduction

### 1.1. Biochar

Biochar is a carbon-rich material known for its stability and long-lasting nature, which refers to its resistance to breakdown or decomposition over long periods of time [1].

From mitigating water pollution to serving as a potential source of energy and combating climate change, biochar has proven to be an invaluable resource in the quest for sustainable solutions [2,3].

Biochar is produced through the pyrolysis process, which involves subjecting biomass or organic waste to high temperatures (ranging from 400 to 600 °C) in the absence of oxygen [4]. During pyrolysis, the biomass is decomposed into three basic components, the solid product, biochar; the liquid, bio-oil, which is formed by the condensation of volatile matters; and the gaseous component, called syngas, which includes carbon monoxide, methane, and carbon dioxide [5–7]. The ratio of these individual components depends on the pyrolysis temperature, heating rate, residence time, etc. [8]. All of these products

originate from cellulose, hemicellulose, and lignin, which is the basic composition of lignocellulosic biomass [9]. The pyrolysis process can be categorized into three classes: slow, fast, and gasification [10]. Due to its ability to produce a higher solid yield (ranging from 25% to 35%) compared to other pyrolysis processes, slow pyrolysis is widely considered as the primary method for biochar production [11]. Biochar International described the stages of pyrolysis [12] as follows: (a) drying and conditioning—at this stage, at ~100 °C, the chemically bound water starts getting driven off the biomass and at above 150 °C, the biomass starts to breakdown; [9] (b) torrefaction—when the biomass is heated to temperatures ranging from 200 to 280 °C, the chemical bonds present in the biomass start to break down, and the formation of oxygen-containing functional groups (OFGs), i.e., hydroxide, carboxyl, carbonyl, lactone, lactol, quinone, chromene, anhydride, phenol, ether, pyrone, pyridine, pyridone, and pyrrole, etc., starts [13]. This process is endothermic, which means that it requires heat input to raise the temperature of the dry biomass and break the molecular bonds; [5] (c) exothermic pyrolysis—at this stage, between 250 and 300 °C, a combustible mixture of gases and tars starts releasing, resulting in cracks, increasing the surface area, and shrinking the particles, and this self-sustaining process keeps on going up to 400 °C, leaving a carbon-enriched residue [14]; however, external heat input is needed to maintain the temperature, and a maximum yield is obtained before the end of exothermic pyrolysis [12]; at this stage, the biochar has an ash content of 1.5–5%, around 25–35% of volatiles, and 60–70% of fixed carbon [12]; (d) endothermic pyrolysis—to increase the fixed carbon content, surface area, and porosity of the biochar, further heating is necessary to decompose more of the volatiles, which is typically achieved at a temperature of 550–600 °C, resulting in a fixed carbon content of 80–85% and a volatile content of 12% [15]; and (e) activation and gasification—at temperatures above 600 °C, a small amount of air and steam can activate the surface of the biochar, increasing its surface area and cation exchange by adding acidic functional groups but reducing its yield through the release of more volatiles [16], or, alternatively, adding more air and/or steam can initiate a gasification process with a low biochar yield (often less than 20%) and high ash content [17]. These physical and chemical properties generated due to varying pyrolysis conditions make biochar a promising tool for a variety of applications. The high surface area and porosity [18,19], presence of oxygen-containing functional groups etc. [17,20] of biochar provide it the benefit of adsorbing a variety of substances, including heavy metals and organic pollutants, making it useful for water treatment [21–23] and soil remediation [10,24]. The high cation exchange capacity of biochar allows it to retain nutrients, making it an effective soil amendment for agriculture [25–29].

### 1.2. Pb(II)

Lead (Pb(II)) is a naturally existing toxic heavy metal of bluish-grey color that is present in trace quantities in the earth's crust and can have serious health consequences when it enters the human body [30].

In the late 1800s, the use of lead pipes for water distribution became increasingly common in major cities across the United States [31]. Even though Pb(II) was more costly compared to iron, the durability and malleability made it a widespread preference for using as pipes [32]. According to the United States Environmental Protection Agency's (USEPA) 7th Drinking Water Infrastructure Needs and Survey Assessment (April 2023) report, there are an estimated number of 9.2 million lead service lines (LSLs) supplying water in US homes [33]. Lead-contaminated drinking water is often the result of corrosion in plumbing materials that contain lead [34]. This is especially common in areas where the water has high acidity or low mineral content, which can cause the corrosion of pipes and fixtures [35].

Children are particularly vulnerable to the harmful effects of lead exposure due to their developing bodies, which absorb more lead than adults [32]. Their brains and nervous systems are also more sensitive to the damaging effects of lead [32]. Children can experience a range of health issues even at low levels of lead exposure, such as behavior and learning

problems, lower IQs, hyperactivity, slowed growth, and hearing problems [36]. In some cases, lead ingestion can also lead to anemia [37]. Severe cases of lead exposure may result in seizures, comas, and even death, although such cases are rare [38]. In adults, lead exposure is linked with harmful effects on cardiovascular health, such as an increased blood pressure and proneness to hypertension [39], deteriorated kidney functions, and reproductive issues in both men and women [40]. Lead exposure in pregnant women is linked to premature births and a reduced growth of the fetus [33]. Replacing the existing lead service lines requires billions of dollars. An ambitious plan was put into place in 2021 to replace all lead service lines within the next ten years under the Bipartisan Infrastructure Law [41]. However, the costs associated with this undertaking are substantial. According to an EPA report, approximately USD 625 billion will be required over the next two decades to address the issues related to drinking water infrastructures [33].

Pb(II) contamination in drinking water has been identified as a significant public health concern, necessitating the exploration of alternative solutions to safeguard human health [42]. Biochar has emerged (as is evident by the numerous articles cited here) as a promising alternative for reducing point-of-use lead concentrations in water [43–46]. In this review, we aimed to capture recent advancements in using biochar for Pb(II) removal from water. We limited our search to studies conducted only from 2012 to 2022 and excluded any research on other metals, soil, or other biosorbents to ensure that our findings were specific to Pb(II), water, and biochar. To compile only the most relevant research within the selected time frame, we used Research Rabbit, a citation-based literature mapping tool for scientific literature that allows for a more targeted search. Figure 1 shows an example of the interface of the tool identifying literature on the relevant topic.

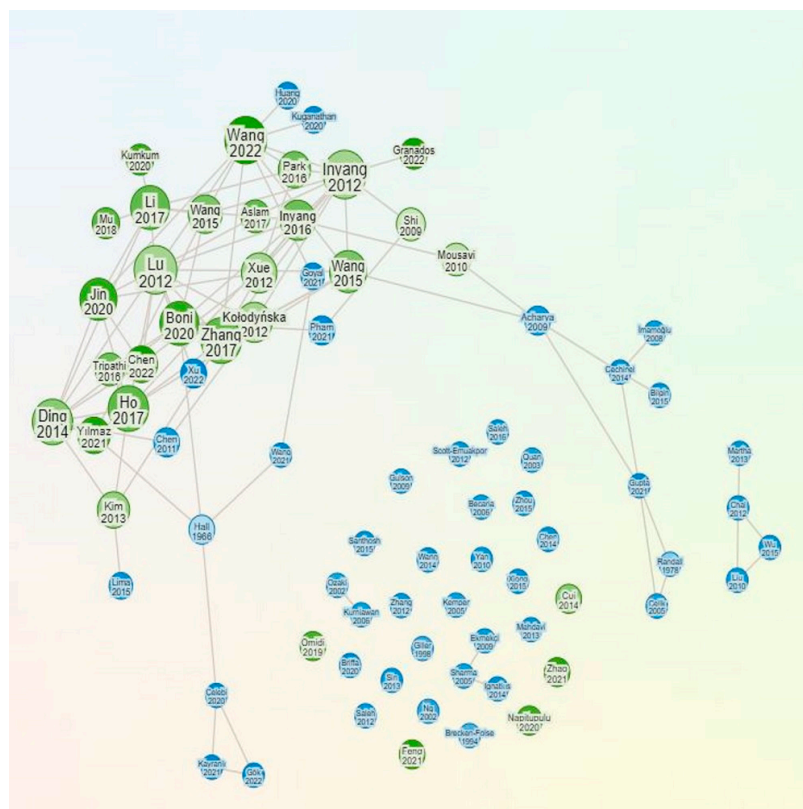


**Figure 1.** Example of the map generated by Research Rabbit to identify the relevant literature [1–14]. Green circles represent the literatures already in the collection and blue circles indicate similar work.

This review article provides several contributions to the field of Pb(II) removal using biochar. Firstly, our study specifically focuses on Pb(II), which allows us to provide additional knowledge in the field of exploring sustainable materials for tackling the Pb(II)-

contamination issue. Additionally, this study discusses the regeneration of Pb(II)-loaded biochar and also the possibility of adsorbed Pb(II) leaching back into the solution by desorption, which has not been typically covered in existing review papers. Furthermore, our study identifies two key gaps in the current literature on the use of biochar for lead removal. Firstly, there is a lack of research on the potential disposal options for Pb(II)-loaded biochar. Secondly, there is a lack of research on column-flow setups, which could provide more knowledge in the real-life application of biochar for Pb(II) removal. By highlighting these gaps and by providing valuable insights, this review article can help guide future research and serve as a vital tool for developing practical solutions to this pressing public health issue.

## 2. Pb(II) Removal Using Pristine Biochar

### 2.1. Feedstock

Researchers have conducted numerous studies to explore the Pb(II)-removing potential of biochar produced from different feedstocks under various pyrolysis conditions. The types of feedstocks they used are agricultural and forest residues, such as wheat and rice [21], wood and bark [21], cinnamon, cannabis [47], sesame straw [22], date seed [48], etc.; industrial by-products, such as anaerobically digested sludge, waste-activated sludge [49], digested whole-sugar beets [50]; and non-conventional materials, such as tire waste [51], etc. The physical and chemical properties of these feedstocks play an important role in defining the adsorption capacity and background mechanism of Pb(II) removal. They appeared to show a high content of oxygen-containing functional groups (OFGs) that provide negatively charged bonding sites on the biochar surface for Pb(II) [52], and some of them have high levels of Na, K, and Mg, which is related to the cation exchange capacity (CEC) and facilitates the ion exchange mechanism when reacting with Pb(II) in a low pH (6.0–7.0) environment [9]. Additionally, the high ash and mineral components present in these biomass feedstocks also promote creating mineral precipitates, which is one of the major dominant mechanisms of removing Pb(II) from water [53].

About 78% of these studies utilized agricultural and forest residues, 18% of these studies explored Pb(II) adsorption by animal waste/industrial by-products, and 4% of these studies investigated non-conventional/synthetic materials as feedstocks to produce biochar to remove Pb(II) from water.

Figure 2 demonstrates the fractions of the different categories of feedstocks utilized to produce biochar.

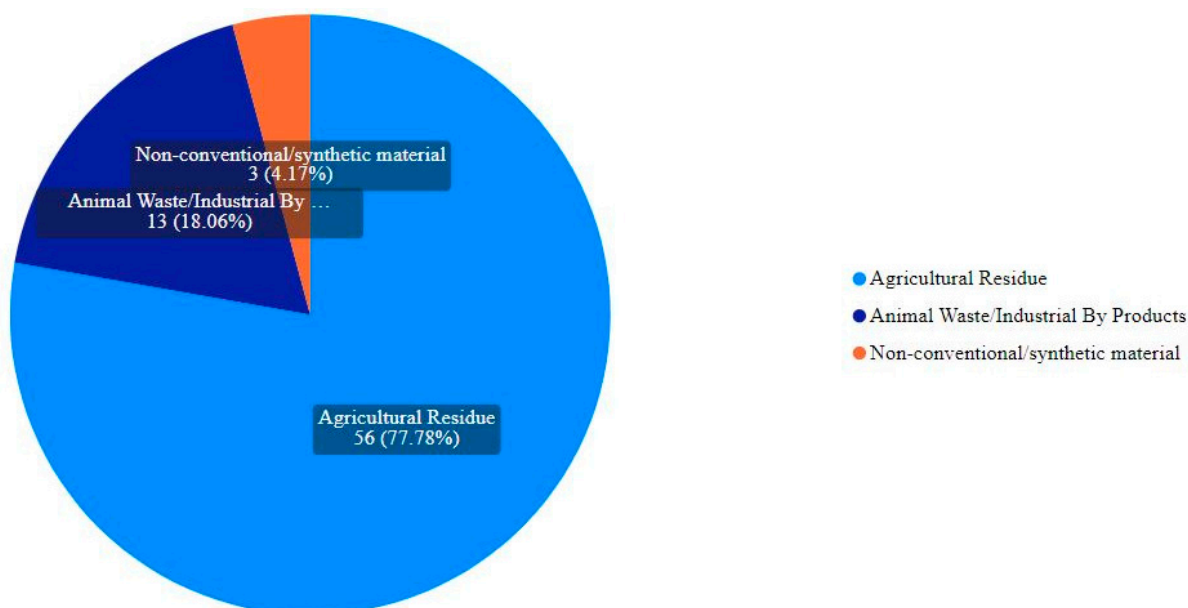


Figure 2. Different categories of feedstocks used for biochar.

## 2.2. Pyrolysis Temperatures/Conditions

A wide range of temperatures (300–700 °C) have been utilized to produce biochar, which resulted in the biochar of various physicochemical properties that played a critical role in removing Pb(II) from water. A low pyrolysis temperature (300–450 °C) typically retains the OFGs, i.e., carboxylic and hydroxylic/phenolic (-COOH, -OH, and C-OH) groups that are present on the biochar surface, which contributes to surface complexation or the electrostatic interaction between biochar and Pb(II) by influencing the protonation and deprotonation of the surface and thereby removing it from the water [21]. As the temperature increases, the volatile matters occupying the pores of the surface starts releasing out of the biomass, creating an increased number of pores and thereby increasing the surface area and pore volume that facilitates the physical adsorption of Pb(II) [47]. Biochar produced by a high pyrolysis temperature showed an increased pH, increased ash/mineral content, decreased number of OFGs, and increased aromaticity and hydrophobicity [4]. These variations in the physicochemical properties correlated with pyrolysis temperatures determine the governing adsorption mechanism.

## 2.3. Experimental Method

Batch experiments and column experiments are two commonly used laboratory methods for studying Pb(II) adsorption using biochar. A batch study is simple and utilizes a static environment. Certain doses of biochar are introduced in a Pb(II)-aqueous solution in reactors of different concentrations. The reactors are then shaken for different reaction times to achieve adequate contact/equilibrium. At the end of the reaction time, the Pb(II) concentration is measured using specific analytical instruments, such as a Flame Absorption Atomic Spectrophotometer (FAAS) or an Inductively Coupled Plasma (ICP) Spectroscopy. Wang et al. investigated the Pb(II)-adsorption potential of biochar from peanut shell and from the residue of Chinese medicine materials [54]. A dosage of 4 g/L of biochar was introduced to a Pb(II) solution of with a concentration of 450 mg/L and 900 mg/L and agitated at 140 rpm on a mechanical shaker. Aliquots were collected at certain time intervals within a duration of 2 to 60 h, and the Pb(II) concentrations were measured in the filtrate using FAAS. The Pb(II)-adsorbed biochar were collected using centrifuge and characterized to study surface-property changes using various analytical instruments, such as a scanning electron microscope (SEM), an energy dispersive spectrometer (EDS), Fourier transform infrared spectroscopy (FTIR), a thermogravimetric analysis (TGA), an X-ray diffractometer (XRD), and X-ray photoelectron spectroscopy (XPS) [49,55]. Batch experiments, following a similar procedure, were conducted by Mu et al., Omididi et al., Zhang et al., and Aslam et al. [19,47,56,57]. For column studies, a fixed bed of the adsorbent, biochar, is set up, and a Pb(II)-aqueous solution of various concentrations passes through, using a peristaltic pump, and samples are collected at different times to measure the concentrations of Pb(II). Ding et al. conducted a column study where hickory wood biochar was used to evaluate the Pb(II)-adsorption potential in a fixed-bed setting [58]. Two layers of quartz sand were used, sandwiching the biochar bed to facilitate the uniform distribution of flow. The column was first flushed with DI water for approximately 2 h, and then the metal solution was employed at the bottom inlet of the column to conduct the flow in an upward direction for 140 min. Aliquots were collected at certain intervals and analyzed to measure the Pb(II) concentration. Column studies appear to provide more realistic results that mimic the real-world scenario of the potential of biochar being used as an adsorbent to remove Pb(II). Fixed-bed filtration systems are frequently utilized in large-scale industrial operations to eliminate pollutants from wastewater streams [21]. In a study conducted by Xue et al., hydrochars packed in laboratory filtration columns were found to be highly effective in removing Pb(II) [59]. However, column studies were performed in only 9% of the reviewed literature. This could be explored further to gain more knowledge and insight regarding the interaction of biochar and Pb(II) in a fixed-bed system.

#### 2.4. Kinetic Modeling

An adsorption process typically involves three steps: (1) the external mass transfer of the adsorbate from the bulk solution to the external surface of the adsorbent, (2) the internal diffusion of the adsorbate to the sorption sites, and (3) the sorption itself. Various models have been developed to describe the kinetics of adsorption, and these models are based on different assumptions about which step is the rate-limiting one [60]. Some models assume that the sorption step is the rate-limiting one, while others assume that the diffusion step is the rate-limiting one. By fitting experimental data to these models, it is possible to determine which step is the rate-limiting one and to gain insights into the underlying mechanisms of the adsorption process. Understanding the rate-limiting step is important for optimizing the design of adsorption systems and for predicting the performance of these systems under different operating conditions [61].

Pseudo-first and pseudo-second order and intraparticle diffusion are the models that typically have been employed [47,62].

According to the pseudo-first order (PFO) kinetic model introduced by Lagergren (1898), adsorption is primarily governed by the difference in the concentration of metal ions in the solution and the adsorbent surface [63]. This model is commonly used to describe the kinetics of metal adsorption in the early stages of the process, assuming that the adsorption occurs via diffusion through the interface. However, this model fails to explain the effect of intraparticle diffusion or other mass transfer limitations that may occur during the later stages of the adsorption process. The pseudo-first order kinetic model equation is as follows:

$$q_t = q_e(1 - e^{-k_1 t}) \quad (1)$$

Here,  $q_t$  = the amount of Pb(II) sorbed at time  $t$ ;

$q_e$  = the amount of Pb(II) sorbed at equilibrium;

$k_1$  = the second-order rate constant.

Physisorption (sorption by intermolecular forces) is the main mechanism involved in this model.

The pseudo-second-order (PSO) model by Ho and McKay (1998) implies that the adsorption rate is dependent on the available adsorption capacity of the adsorbent and not on the concentration of the adsorbate itself [64]. This model considers that the rate at which adsorption sites are filled is directly proportional to the square of the number of available activated sites on the surface of the adsorbent. This suggests that the rate of adsorption is limited by the number of available adsorption sites on the adsorbent surface rather than the concentration of the adsorbate in the solution. Therefore, this model can be applicable to the entire timeline of the sorption process, especially when chemisorption is the rate-limiting mechanism [21]. The pseudo-second-order equation can be written as follows:

$$q_t = \frac{k_2 q_e^2 t}{1 + k_2 q_e^2 t} \quad (2)$$

Here,  $q_t$  = the amount of Pb(II) sorbed at time  $t$ ;

$q_e$  = the amount of Pb(II) sorbed at equilibrium;

$k_2$  = the second-order rate constant.

The Elovich model assumes that the rate of adsorption of a solute decreases exponentially as the amount of adsorbed solute increases. This indicates that as more solute is adsorbed onto the surface of the adsorbent material, the availability of active sites on the surface decreases, leading to a slower adsorption rate. Despite its initial development for gaseous systems, the Elovich model has proven to be a useful tool for understanding the kinetics of adsorption in wastewater processes and for predicting the performance of adsorption systems under different operating conditions [65]. The model can be expressed by Equation (3):

$$q_t = \frac{1}{\beta} = \ln(\alpha\beta t + 1) + b \quad (3)$$

Here,  $q_t$  = the amount of Pb(II) sorbed at time  $t$ ;

$\alpha$  = the initial adsorption rate;

$\beta$  = the desorption constant at time  $t$ .

The intraparticle diffusion model is a useful tool for describing adsorption processes in which the rate of adsorption is influenced by the rate of diffusion of the adsorbate towards the adsorbent surface [66]. This suggests that the process is controlled by the diffusion rate of the adsorbate [18]. The equation can be expressed as Equation (4):

$$q_t = k_3 t^{\frac{1}{2}} + b \quad (4)$$

Here,  $q_t$  = the amount of Pb(II) sorbed at time  $t$ ;

$k_3$  = the intraparticle diffusion rate constant;

$b$  = the intercept.

After fitting the experimental data with this model, the resulting value of  $b$  indicates how the thickness of the boundary layer of the biochar can influence the adsorption process [54].

Table 1 summarizes the different kinetic models investigated in the reviewed studies, along with the corresponding feedstocks, pyrolysis conditions, and pre-/post-treatments.

### 2.5. Isotherm Modeling

Researchers have adopted mathematical approaches, such as isotherm models, to study the adsorption behavior of Pb(II) onto biochar under different conditions, such as a differing pH, temperature, initial Pb(II) concentration, flow, etc. [67,68]. There are several different isotherm models that are used by researchers including the Langmuir, Freundlich, Temkin, Thomas, Yoon–Nelson, Bohart–Adams, Prausnite–Radke, Redlich–Peterson, Toth, and Sips isotherms, etc. [48,69]. Each of these models has a different mathematical form and is used to describe different aspects of the adsorption behavior.

The Langmuir isotherm model is a commonly used approach for characterizing the adsorption of solutes onto solid surfaces [70,71]. This model is based on the assumption that the adsorbent surface is uniform and homogeneous in nature, which means that all the adsorption sites have the same energy [72]. Additionally, the model assumes that there is no interaction between adsorbed molecules on different sites and that each site can accommodate only one adsorbed molecule at a time [51].

By utilizing the Langmuir isotherm model, it is possible to gain insights into the adsorption process and obtain essential information about the adsorption capacity of the adsorbent material, the affinity of the adsorbate for the adsorbent surface, and the maximum adsorption capacity of the adsorbent [50,54]. This information can be used to optimize the design and operating conditions of adsorption systems and ensure their optimal performance. The model can be expressed as Equation (5):

$$q_e = \frac{q_{max} K_L C_e}{1 + K_L C_e} \quad (5)$$

Here,  $q_{max}$  = the maximum amount of adsorbed Pb(II) by the unit weight of biochar;

$q_e$  = the amount of Pb(II) adsorbed at an equilibrium concentration;

$K_L$  = the Langmuir constant;

$C_e$  = the concentration of Pb(II) in the solution at equilibrium.

The Freundlich isotherm model assumes that the adsorbent surface is heterogeneous and that adsorption happens in a multilayer sorption, where adsorbate molecules tend to preferentially attach to sites that have a stronger affinity (higher bonding energy) for them, resulting in the formation of multiple layers of the adsorbate molecules on the adsorbent surface [21]. In contrast to the Langmuir model, this model accounts for the non-uniform distribution of the adsorption heat and affinity toward the heterogeneous

surface. It assumes that the adsorption process occurs on sites with varying properties, resulting in a non-uniform distribution of the adsorption [73]. The Freundlich equation can be expressed as Equation (6):

$$q_e = K_F C_e^n \quad (6)$$

Here,  $q_e$  = the amount of Pb(II) adsorbed at an equilibrium concentration;  
 $K_F$  = the adsorption coefficient of the Freundlich model.

Table 1 summarizes the different isotherm models investigated in the reviewed studies, along with the corresponding feedstocks, pyrolysis conditions, and pre-/post-treatments.

## 2.6. Sorption Mechanisms

The adsorption and removal of Pb(II) from water by biochar involves various mechanisms, including surface complexation, electrostatic interaction/ion exchange, and mineral precipitation.

### 2.6.1. Physical Sorption

Biochar is composed of micropores (<2 nm), mesopores (2–50 nm), and macropores (>50 nm), which have the capacity to capture Pb(II) ions and remove them from the solution through the process of physical sorption [74]. The amount of Pb(II) adsorbed onto these sites is determined by the number of available sites, which is influenced by the type of feedstock used and the pyrolysis temperature during biochar production [6]. The unique pore structure of biochar provides a large surface area for adsorption, making it an effective adsorbent for Pb(II) removal. Physical sorption occurs as Pb(II) ions are attracted to and captured by the available sites within the biochar pores [75]. This process is influenced by various factors, such as the size and shape of the pores [15], the chemical composition of the biochar, and the concentration of Pb(II) ions in the solution [76–78]. The pore volume and surface area of biochar can be quantified using a BET surface analyzer [79]. Increasing the temperature during pyrolysis leads to an increase in the specific surface area [80]. This happens when the volatile matters present in the feedstock starts escaping the pores as the temperature increases and, therefore, the surface area increases [81]. However, a non-woody biomass appeared to have high nutrient and ash contents, which volatilized and increased the surface area and porosity of biochar under a high pyrolysis temperature [57]. While it is generally true that elevating the temperature to above 400 °C can lead to an increase in the surface area, there have been some studies that have observed the opposite effect. This can be attributed to factors such as tar blocking the pores, partial ash fusions, or a decomposition of the porous structure [82,83].

### 2.6.2. Surface Complexation with Functional Groups

This process is facilitated by the presence of oxygen-containing functional groups on the biochar surface, which can be identified by Fourier Transform Infrared Spectroscopy (FTIR). The presence and position of carboxyl and hydroxyl groups in the FTIR spectrum can provide insights into their role in the adsorption process. The content of these functional groups is dependent on the feedstock properties of the biochar, the pyrolysis conditions, and the pH of the solution. Although a woody biomass has a lower surface area compared to a non-woody biomass, the presence of OFGs makes it favorable for them to adsorb Pb(II) from water. These woody biomasses, and also agricultural and forest residues, have an abundant amount of oxygen-containing groups (carboxyl COOH, carbonyl C=O, and hydroxyl OH) that provide negatively charged surface binding sites and that facilitate creating surface complexation with Pb(II) [53,77,84].

These functional groups participate in the cation exchange mechanism, whereby they either gain protons (at a low pH) or donate protons (at a high pH) in the presence of Pb(II) [20]. The extent of cation exchange is determined by the concentration of the exchangeable cations on the biochar surface and their affinity for the adsorbed cations [4]. The content of the functional groups in biochar decreases with temperature due to higher

carbonization [76]. This is because the dehydration of cellulose and lignin begins at 300 °C, and their transformation occurs at 400 °C [83].

### 2.6.3. Electrostatic Interaction

Pb(II) adsorption by electrostatic interaction occurs when positively charged Pb(II) ions are attracted to the negatively charged surface of the biochar [49,85]. This attraction is due to the electrostatic forces between the ions and the surface [50]. When the biochar has a net negative charge, it can attract and bind positively charged ions, such as Pb(II) [86]. The strength of this interaction depends on the magnitude of the charge on the biochar surface, the size and charge of the ions, and the ionic strength of the solution [29,85]. When the pH of the net solution is zero, no interaction happens [47]. But when the pH of the solution is greater than the pH at the point of zero charge (pHPZC) [83], then the biochar surface becomes negatively charged by releasing H<sup>+</sup> and facilitates the adsorption of the positively charged Pb(II) [87]. When the pH of the solution is less than the pH at the point of zero charge, then the biochar surface becomes positively charged by gaining H<sup>+</sup> and repulsing the positively charged Pb(II) [19]. At a high pyrolysis temperature (>500 °C), the content of the negatively charged surface functional groups decreases, causing a reduction in the negative surface charge and an increase in the pH at the point of zero charge [83]. Also, a high temperature increases the ash content, which facilitates an increase in the pH of the solution when the biochar is introduced [83]. Similarly, a low pyrolysis temperature is attributed with a high amount of oxygen functional groups, which thereby promotes an increased chance of surface complexation [88].

### 2.6.4. Mineral Precipitation

Pb(II) adsorption by mineral precipitation occurs when these ions react with the minerals present in the biochar to form insoluble precipitates [19]. The formation of these precipitates is influenced by several factors, including the pyrolysis temperature and the mineralogy and surface chemistry of the biochar [89]. Biochar with an alkaline nature [90], which is produced by the thermal degradation of cellulose and hemicellulose at temperatures above 400 °C, can facilitate the precipitation of metals [91]. Also, biochar derived from animal waste is rich in minerals such as Ca and K, which can participate in the precipitation of metals on the biochar surface [91]. Mineral components can take part in removal through a competitive ion exchange as well [83]. Increasing the temperature during biochar production leads to a higher content of mineral components [4,80]. However, the water-soluble fraction of these minerals stops increasing beyond 200 °C. This is due to the fact that at temperatures above 200 °C, the minerals start to crystallize [92], resulting in reduced solubility. This is attributed to the facilitation of the removal of Pb(II) through mineral precipitation [83].

### 2.6.5. Ion Exchange

Cation exchange is another important mechanism that plays a role when removing Pb(II) from water using biochar [18,93]. Biochar properties consist of cations such as Na, K, Ca, Mg, etc. [9]. While in a solution, these are released, and due to the competitive affinity of different ions on the binding active sites of biochar, Pb(II) ions may be exchanged with these mineral ions and thereby may be removed from the solution [72,87]. High levels of Na, K, and Mg are associated with an increased Cation Exchange Capacity (CEC). A high CEC promotes ion exchange under acidic pH by the biochar releasing these in the solution and creating bonding with Pb(II) [53,94]. Figure 3 demonstrates the different sorption mechanisms, and Table 1 summarizes the key findings of the different studies.

**Table 1.** Removal mechanisms and key findings: Pb(II) removal using pristine biochar.

Feedstock	Production Method/ Pyrolysis Condition	Removal Mechanism/Kinetic Model/Isotherm Model	Maximum Adsorption	Key Findings/Notes	Reference
Carbon Wheat Straw and Natural Straw	300 °C for 60 min	<ul style="list-style-type: none"> <li>Langmuir</li> <li>PSO</li> <li>Endothermic</li> </ul>	149.7 mg/g	<ul style="list-style-type: none"> <li>Increased dosage of biochar showed increased Pb(II)-removal percentage.</li> <li>Adsorption Capacity<sub>Carbon wheat straw</sub> &gt; Adsorption Capacity<sub>Natural straw</sub>.</li> <li>Carbon wheat straw biochar reached equilibrium faster than natural straw.</li> </ul>	[56]
Cinnamon cannabis	300, 400, and 600 °C for 120 min	<ul style="list-style-type: none"> <li>Surface complexation</li> <li>Ion exchange</li> <li>Electrostatic interaction</li> <li>Langmuir</li> </ul>	135.68–168.05 mg/g	<ul style="list-style-type: none"> <li>Increased pyrolysis temperature resulted in higher surface area.</li> <li>Average pore size indicated that adsorbent has mesoporous structure.</li> </ul>	[47]
<i>Phyllostachys pubescens</i> (PP)	0–4% oxygen content atmosphere—slow pyrolysis—450 °C and 700–60 min	<ul style="list-style-type: none"> <li>Precipitation</li> <li>Surface complexation through Pb(II)-<math>\pi</math> interaction and functional groups</li> </ul>	67.4 mg/g	<ul style="list-style-type: none"> <li>Increased oxygen content showed increased contribution of mineral precipitation in Pb(II) removal.</li> <li>Increase in pyrolysis temperature increased surface area, porosity through aromatization (related to decreased functional groups), and <math>\pi</math> chemical bond.</li> <li>Under an oxygen-rich atmosphere and low pyrolysis temperature (450 °C), the lactonic functional group (i.e., carboxylic esters), pore volume, and surface area of the pyrolysis product increased, which in turn created additional adsorption sites.</li> <li>As the temperature increased, the number of oxygen-containing functional groups decreased, while the ash content increased. The ash was composed of various inorganic compounds, including calcium carbonate, which aided in the precipitation-based removal process.</li> </ul>	[19]

Table 1. Cont.

Feedstock	Production Method/ Pyrolysis Condition	Removal Mechanism/Kinetic Model/Isotherm Model	Maximum Adsorption	Key Findings/Notes	Reference
Rice husk Dairy manure	350 °C for 4 h	<ul style="list-style-type: none"> <li>• Surface complexation</li> <li>• Precipitation</li> </ul>	Not quantified	<ul style="list-style-type: none"> <li>• The decomposition of cellulose and hemicellulose in rice husk biochar occurred at a temperature of around 300 °C, resulting in the production of organic acid and phenolic compounds that can cause a decrease in pH.</li> <li>• Dairy manure biochar exhibited a higher pH level, owing to the minerals that initiate separation beyond the temperature threshold of 300 °C.</li> <li>• The adsorption characteristics of the multimetal solution were not the same as those of the monometal.</li> </ul>	[29]
Sesame straw	700 °C for 4 h	<ul style="list-style-type: none"> <li>• Langmuir</li> </ul>	<ul style="list-style-type: none"> <li>• 102 mg/g (monometal)</li> <li>• 88 mg/g (multimetal)</li> </ul>	<ul style="list-style-type: none"> <li>• Among the cations present in the multimetal solution, Pb(II) exhibited the highest level of adsorption. This aligns with the results of other studies.</li> <li>• Adsorption capacity increased with the increase in temperature, which means this was an endothermic process.</li> </ul>	[22]
Peanut hull	450 °C	<ul style="list-style-type: none"> <li>• Surface complexation</li> <li>• Precipitation</li> <li>• Electrostatic interaction</li> </ul>	63.09 mg/g	<ul style="list-style-type: none"> <li>• The adsorption capacity was found to be greater in particles with a size of less than or equal to 2 mm compared to those with a size greater than 2 mm. This is due to the fact that smaller particle sizes have a larger surface area, which facilitates greater adsorption.</li> </ul>	[72]

Table 1. Cont.

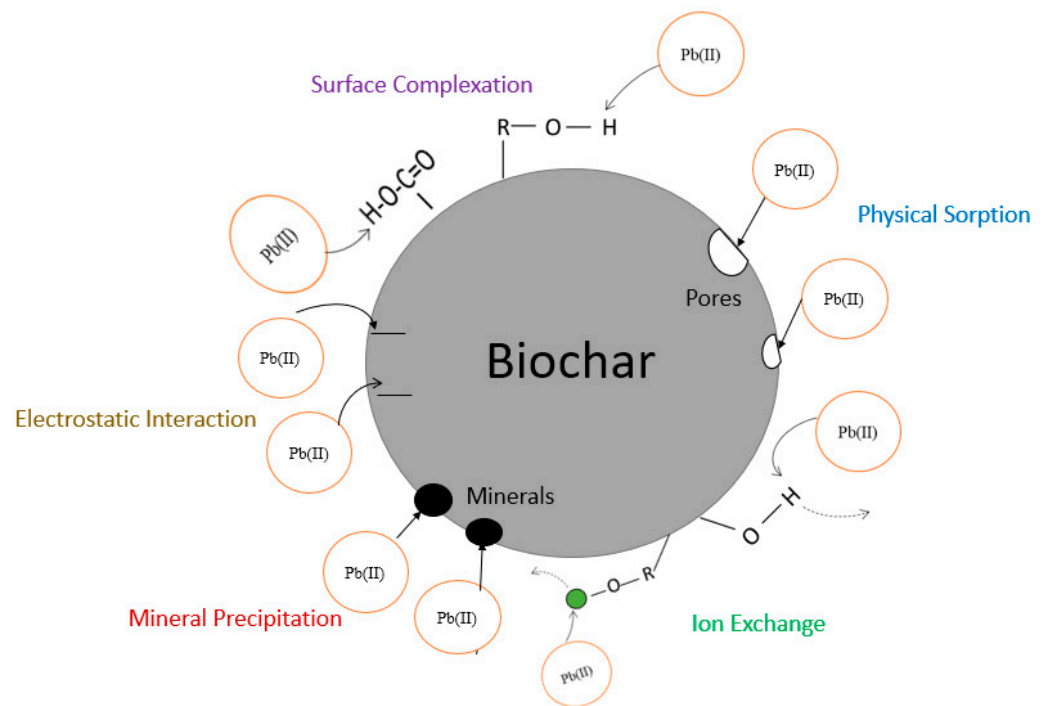
Feedstock	Production Method/ Pyrolysis Condition	Removal Mechanism/Kinetic Model/Isotherm Model	Maximum Adsorption	Key Findings/Notes	Reference
<ul style="list-style-type: none"> <li>Avocado seed</li> <li>Avocado peel</li> <li>Grapefruit peel</li> <li>Brown seaweed</li> </ul>	<ul style="list-style-type: none"> <li>Laboratory tube furnace (300 °C 1 h)</li> <li>DIY biochar maker (BioCharlie Log—ASB, APB, GPB, and BSB)</li> </ul>	<p>This study did not discuss the adsorption mechanism, but the authors guessed the chemisorption processes—precipitation, ion exchange, electrostatic attraction, and surface complexation. However, in this study is unique in a sense that the authors compared lab-made biochar and home-made (temperature uncontrolled) biochar</p>	Not quantified; used % removal	<ul style="list-style-type: none"> <li>Land-based biochar (Avocado and Grapefruit): high carbon content, and oxygen-containing functional groups were the dominating factor in Pb(II) adsorption.</li> <li>Marine-based biochar (seaweed): high ash content, which played a governing role in adsorption.</li> <li>The typical trend of an increased pH with an increased pyrolysis temp was not found in this study, which the authors attributed with the biomass-specific characteristics.</li> <li>Lab-produced biochar showed better adsorption efficiency.</li> <li>In this study, the authors discussed the correlation between the O:C ratio and biochar stability, which is not quite typical with regards to the discussion points of other studies.</li> </ul>	[62]
<ul style="list-style-type: none"> <li>Green waste biochar (GWB) (consists of Bermuda Grass—Cynodondactylon)</li> <li>Poplar twigs biochar (PTB)</li> </ul>	350 °C and 650 °C at 8–9 °C min <sup>-1</sup>	<ul style="list-style-type: none"> <li>Surface complexation</li> <li>Precipitation</li> <li>Cation exchange</li> </ul>	44.42 mg/g	<ul style="list-style-type: none"> <li>A higher pH was found for a higher temp, which is in agreement with other studies that suggest that a high pH is associated with a low O and H and a low amount of oxygen functional groups.</li> <li>A low temp and a high CEC were found as well as a high surface area and a high amount of functional groups, which is because at a high temp, oxygen-containing functional groups become volatilized.</li> </ul>	[57]
Grape pomace	300–700 °C at 10 °C min <sup>-1</sup>	<ul style="list-style-type: none"> <li>Physisorption and chemisorption</li> </ul>	134 mg/g	Uniqueness: experiment with low Pb(II) concentration to mimic practical scenarios.	[87]

Table 1. Cont.

Feedstock	Production Method/ Pyrolysis Condition	Removal Mechanism/Kinetic Model/Isotherm Model	Maximum Adsorption	Key Findings/Notes	Reference
<ul style="list-style-type: none"> <li>Waste-activated sludge</li> <li>Anaerobic digestion sludge</li> </ul>	400–800 °C at 15 °C min <sup>-1</sup>	<ul style="list-style-type: none"> <li>Precipitation (dominant: 53.5%)</li> <li>Ion exchange</li> <li>Surface complexation</li> <li>Electrostatic interaction</li> </ul>	53.96 mg/g	<ul style="list-style-type: none"> <li>The ion exchange capacity and precipitation tendency were found to be higher in the biochar prepared at a higher temperature, as compared to those prepared at a lower temperature (400 °C). Additionally, the biochar prepared at a lower temperature contained fewer functional groups than the biochar prepared at 800 °C. These findings are in agreement with other studies.</li> <li>At high temperatures, low H:C and O:C ratios indicated a high carbon content due to increased carbonization and aromaticity, resulting in greater resistance to decomposition. This means that a high temperature provides increased thermal stability.</li> </ul>	[49]
<ul style="list-style-type: none"> <li>Peanut shell</li> <li>Residue of Chinese medicine materials</li> </ul>	300–600 °C	<ul style="list-style-type: none"> <li>Surface complexation</li> <li>Pb(II)–<math>\pi</math> interaction</li> <li>Precipitation</li> </ul>	82.5 mg/g	<ul style="list-style-type: none"> <li>For the peanut shell, the adsorption efficiency was higher with low temperatures and the medicine residue biochar showed higher adsorption efficiency with high temperatures.</li> <li>Precipitation was the dominant mechanism in all cases, except Pb(II)–<math>\pi</math> interactions in the peanut shell biochar which was the dominant one with a high temp.</li> </ul>	[54]
Sugarcane bagasse	250, 400, 500, and 600 °C at 10 °C min <sup>-1</sup>	<ul style="list-style-type: none"> <li>Surface complexation</li> <li>Precipitation</li> </ul>	21 mg/g	<ul style="list-style-type: none"> <li>Sorption capacity decreased with increasing temp.</li> </ul>	[95]

Table 1. Cont.

Feedstock	Production Method/ Pyrolysis Condition	Removal Mechanism/Kinetic Model/Isotherm Model	Maximum Adsorption	Key Findings/Notes	Reference
Sludge	550 °C for 2 h	<ul style="list-style-type: none"> <li>• Surface complexation</li> <li>• Precipitation</li> <li>• Ion exchange</li> </ul>	30.88 mg/g	<ul style="list-style-type: none"> <li>• Presence of carboxyl and hydroxyl groups facilitated co-ordination with Pb(II) by acting as a proton donor.</li> <li>• Higher pH levels created more sites for surface complexation, since more carboxylic groups deprotonated and thus helped in sorption.</li> <li>• As the pH level rose beyond 5, co-precipitation mechanisms started playing their roles.</li> </ul>	[96]
Wheat straw	400 °C for 2 h	<ul style="list-style-type: none"> <li>• Surface complexation</li> </ul>	185.19 mg/g	<p>This study explored the potential of hydroxide complex formation at higher pH levels, although it did not delve into the possibility of metal precipitation as a result of this mechanism.</p> <ul style="list-style-type: none"> <li>• Somewhat similar FTIR spectra of pre- and post-sorption indicated that lead adsorption was not governed by an interaction with the surface functional groups.</li> </ul>	[85]
<ul style="list-style-type: none"> <li>• Digested animal waste</li> <li>• Digested whole sugar beet</li> </ul>	600 °C for 2 h	<ul style="list-style-type: none"> <li>• Precipitation</li> </ul>	200 mg/g	<ul style="list-style-type: none"> <li>• Even though Pb(II) had the highest surface electronegativity compared to other metals, it still did not show the highest tendency for adsorption. This is not in agreement with other studies [23].</li> </ul>	[50]
Red fruit peel	300 °C for 2 h	<ul style="list-style-type: none"> <li>• Physical sorption</li> </ul>	61.86 mg/g	<ul style="list-style-type: none"> <li>• This study found that a higher ash content led to lower adsorption rates, likely due to clogging of the biochar pores.</li> <li>• These researchers also observed a peak in adsorption, followed by a decrease, which they attributed to desorption, since adsorption is a reversible process.</li> </ul>	[86]



**Figure 3.** Sorption mechanisms involved in Pb(II) removal.

Omidi et al. investigated the adsorption of Pb(II) by biochar using cinnamon and cannabis as feedstocks [47]. Similar to other studies, they also found that the adsorption capacity increases with an increase in the biochar dose until a certain point, after which it starts to decrease. This can be attributed to the fact that, initially, there are numerous bonding sites available which get occupied rapidly, leading to an increase in the adsorption capacity. However, as the dose is further increased, the rate of available active sites exceeds the rate of adsorption, resulting in a decrease in capacity. To strike a balance between these two factors, an optimum dose was identified. In this study, the increase in the initial concentration of Pb(II) was observed to enhance the adsorption capacity while reducing the removal percentage. This can be attributed to the higher availability of the adsorbate for adsorption. However, since more ions are available for adsorption, the rate at which they get adsorbed decreases, leading to a reduction in the removal percentage. The adsorption rate happened to be faster in the initial stage of reaction due to the abundance of active binding sites, and, as time progresses, the number of available sites for adsorption decreases as they become occupied. Consequently, the rate of adsorption reduces [47]. A further analysis of how functional groups affect the adsorption process could have greatly enhanced the value of this research.

Xu et al. conducted their comparative adsorption study using rice husk (RHBC) and dairy manure biochar (DMBC) [29]. DMBC is more effective than RHBC in removing Pb(II) due to its ability to use both ionized phenolic O- group complexation and mineral precipitation with  $\text{CO}_3^{2-}$  and  $\text{PO}_4^{3-}$ . In contrast, RHBC only utilizes complexation with ionized phenolic O- groups to remove metal. These researchers examined the sorption of metals in mono- and multimetal solutions and at low and high metal concentrations. They discovered that RHBC exhibited greater competition in both low and high concentrations due to its reliance on a single mechanism—complexation with phenolic groups. Meanwhile, DMBC was less affected by competition due to its ability to use multiple mechanisms. The competition was greater for both types of biochar in the high concentration, because more metals compete for the available sites [29]. Cui et al. investigated Pb(II) adsorption using peanut hull-derived biochar [72]. This study explored the effects of the particle size of biochar on the adsorption process, which is not a very typical practice. The adsorption

capacity showed a similar pattern of increase with an increasing pH, until it reached a pH of 5.5. After 5.5, the rate of the capacity increase slowed down and reached equilibrium. However, the adsorption capacity remained high due to the precipitation mechanism, in addition to complexation. These results align with findings from other studies.

Wang et al. explored the adsorption of Pb(II) using peanut shell and the residue of Chinese medicine materials as biochar feedstocks [54]. In this study, a weak correlation was found between the reduction in Pb(II) sorption and ash content. The results suggest that precipitation is not solely dependent on the mineral content, which is different from the findings of other studies. Instead, the morphology of minerals, specifically the crystallization of minerals, was found to have an influence on the adsorption of Pb(II).

### 3. Pb(II) Removal by Modified/Functionalized Biochar

Researchers have explored the removal of Pb(II) by modifying or functionalizing biochar to either increase the removal capacity or to target specific contaminants, which shows a low adsorption potential by pristine biochar. They have studied modifications by metal oxides, such as hydrous manganese oxide (HMO) [97], MnO<sub>2</sub> [98], and KMnO<sub>4</sub> [99], and metal salts, such as MgCl<sub>2</sub> [100,101], FeCl<sub>3</sub> [102,103], MnSO<sub>4</sub>, and KHCO<sub>3</sub> [104]. They have also studied activations by gases, such as CO<sub>2</sub> [105], and complex organics like chitosan [106], as well as modifications by nanoparticle composites, such as ZnO [107] and nanoscale Zero-Valent Iron (nZVI) [108]. These studies were able to show a 2–49-time increase in adsorption capacity.

Figure 4 demonstrates that a majority of the studies utilized metal salts or oxides for modifying the biochar. Table 2 summarizes the key findings of the different studies.

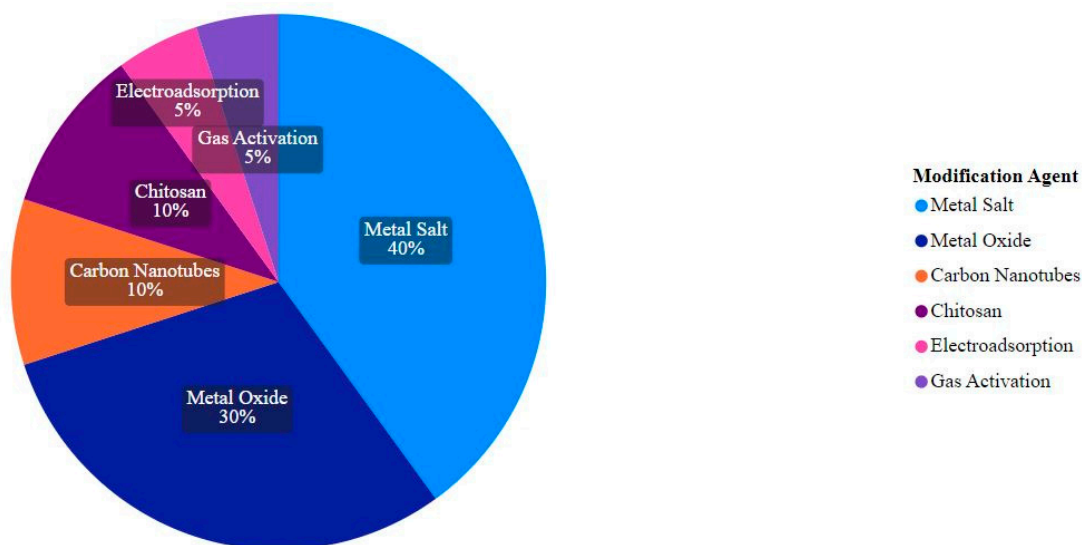


Figure 4. Different modification agents used for functionalizing biochar.

Table 2. Removal mechanisms and key findings: Pb(II) removal using modified biochar.

Feedstock	Modifying Agent/Compound	Pre-Pyrolysis/ Post-Pyrolysis	Production Method	Sorption Increase	Maximum Adsorption	Removal Mechanism/Kinetic Model/Isotherm Model	Key Findings/Notes	Reference
Pinewood	Hydrous manganese oxide (HMO)	Post	Feedstock was first converted to biochar by pyrolysis—100 °C for 1 h and then 700 °C for 3 h. Prepared biochar was then modified by manganese nitrate and KMnO <sub>4</sub> .	92.50%	Not specified	<ul style="list-style-type: none"> <li>• Surface complexation</li> <li>• Electrostatic interaction</li> <li>• PSO (rate was proportional to the number of active sites)</li> <li>• Langmuir</li> <li>• Endothermic (with an increased temperature, sorption increased)</li> <li>• Ion exchange</li> <li>• Mineral precipitation</li> <li>• Interaction with OFGs</li> <li>• Metal-<math>\pi</math> electron co-ordination</li> <li>• Langmuir</li> </ul>	Modification increased the number of hydroxyl groups, decreased pH at point of zero charge (pH <sub>PZC</sub> ), and increased the number of mesopores and macropores.	[97]
Coconut shell	MgCl <sub>2</sub>	Pre	Feedstock was first impregnated with MgCl <sub>2</sub> and then pyrolyzed at 400 °C.	20 times	532.28 mg/g	<ul style="list-style-type: none"> <li>• Freundlich</li> <li>• PSO</li> </ul>	Modification increased the OFG content.	[55]
Corn straw	MgCl <sub>2</sub>	Post	Feedstock was first converted to biochar by pyrolysis—250 °C for 2 h. Prepared biochar was then modified by MgCl <sub>2</sub> .	More than 2 times	5.15 mg/g	<ul style="list-style-type: none"> <li>• Electrostatic interaction</li> <li>• Surface complexation</li> <li>• Ion exchange</li> </ul>	Physical/chemical property changes associated with the modification were not investigated. No comparative analysis based upon the characteristic features were explored.	[101]
Swine manure	MnO <sub>2</sub>	Post	Feedstock was first converted to biochar by pyrolysis—400 °C for 2 h. Prepared biochar was then modified by KMnO <sub>4</sub> .	2 times	268 mg/g	<ul style="list-style-type: none"> <li>• PSO</li> <li>• Langmuir–Freundlich</li> <li>• Endothermic</li> </ul>	Adsorption was dependent on pH, which is similar to other studies. Modification increased the surface area and pore volume.	[98]
Oak wood and Oak bark	Metal salt impregnation followed by alkali (NaOH) treatment	Post	Fe <sub>2</sub> (SO <sub>4</sub> ) <sub>3</sub> ·nH <sub>2</sub> O and FeSO <sub>4</sub> were used to make Fe <sup>2+</sup> /Fe <sup>3+</sup> SO <sub>4</sub> <sup>2-</sup> , 400–450 °C. Fast pyrolysis.	2.5 times	55.91 mg/g	<ul style="list-style-type: none"> <li>• PSO</li> <li>• Langmuir–Freundlich</li> <li>• Endothermic</li> </ul>	Introduction of iron oxide on the surface of biochar influenced the adsorption process.	[109]
Antibiotic residue	CO <sub>2</sub> gas activation	During pyrolysis	300–800 °C for 2 h	3 times	454 mg/g	Highest Pb(II) adsorption occurred by the biochar produced at 700 °C	Study focused on increasing the carbon and ash component (carbonate and phosphate) of biochar to improve Pb(II) removal through mineral precipitation.	[105]

Table 2. Cont.

Feedstock	Modifying Agent/Compound	Pre-Pyrolysis/ Post-Pyrolysis	Production Method	Sorption Increase	Maximum Adsorption	Removal Mechanism/Kinetic Model/Isotherm Model	Key Findings/Notes	Reference
Lotus leaf	(NH <sub>4</sub> ) <sub>2</sub> HPO <sub>4</sub> (diammonium hydrogen phosphate)	Pre	600 °C for 1 h	2 times	1936.2 mg/g	<ul style="list-style-type: none"> <li>• Freundlich</li> <li>• Complexation and precipitation</li> </ul>	Modified biochar (NP-BC) had -COOH, -NH <sub>2</sub> , P=O, and -OH, which co-ordinated with Pb(II) to form complexation. Electro-assistance improved adsorption by increasing the surface charge density and bringing ions into closer contact with the biochar.	[110]
Date seed	Electro-adsorption	Post	Pyrolyzed biochar was used as an electrode—550 °C for 3 h	21%	179.64 mg/g	<ul style="list-style-type: none"> <li>• Electrostatic interaction</li> <li>• Physical adsorption</li> <li>• Surface complexation</li> </ul>	Additionally, the electric current increased the pore structure.	[111]
Rice husk	Metal salt and metal oxide: rice husk biochar (BC) ---> magnetic rice husk biochar (FBC) ---> KMnO <sub>4</sub> -treated magnetic biochar (FMBC)	Pre and post	Pre-pyrolysis (600 °C for 1.5 h) magnetization and post-pyrolysis (600 °C for 0.5 h) KMnO <sub>4</sub> activation.	7 times	148 mg/g	<ul style="list-style-type: none"> <li>• Surface complexation</li> <li>• PSO</li> <li>• Langmuir</li> </ul>	KMnO <sub>4</sub> treatment increased OFGs, because KMnO <sub>4</sub> oxidized and produced more OFGs, and MnO has a greater affinity for heavy metals (HMs).	[79]
Cassava root husk	ZnO Nanoparticles	Post	Pyrolysis (400 °C for 2 h) and wet impregnation.	28% or 1.39 times	42.05 mg/g	<ul style="list-style-type: none"> <li>• Precipitation</li> <li>• Surface complexation</li> </ul>	Modification increased the number of -OH, which dropped after adsorption, indicating that precipitation took part in Pb(II) removal. It also increased the -CO- that took part in surface complexation. Modification reduced aromaticity, which is favorable for Pb(II) adsorption.	[107]
Sugarcane straw	FeCl <sub>3</sub>	Post	Pyrolysis: 350 and 750 °C at 5 °C min <sup>-1</sup> . Modification: wet impregnation.	2–11%	92.81 mg/g	<ul style="list-style-type: none"> <li>• Precipitation (due to higher ash content)</li> <li>• Electrostatic interaction</li> </ul>	Modification increased the specific surface area and exposed functional groups.	[102]

Table 2. Cont.

Feedstock	Modifying Agent/Compound	Pre-Pyrolysis/ Post-Pyrolysis	Production Method	Sorption Increase	Maximum Adsorption	Removal Mechanism/Kinetic Model/Isotherm Model	Key Findings/Notes	Reference
<ul style="list-style-type: none"> <li>Nut shield</li> <li>Wheat straw</li> <li>Grape stalk</li> <li>Grape husk</li> </ul>	FeCl <sub>3</sub>	Post	Pyrolysis: 600 °C for 30 min. Modification: wet impregnation.	461%	179 mg/g	<ul style="list-style-type: none"> <li>Surface complexation</li> </ul>	Magnetization increased sorption by improving the structure of biochar. Fe oxides promoted stronger chemical bonds with Pb(II). Fe oxides increased CEC value significantly, and CEC is an important feature for Pb(II) adsorption.	[103]
Raw cypress sawdust (RCS)	MgCl <sub>2</sub>	Pre	600 °C for 1 h	7.4 times	202.2 mg/g	<ul style="list-style-type: none"> <li>Surface complexation</li> <li>Precipitation</li> </ul>	Modification increased the surface area, amount of OFGs, and the CEC associated with Mg ions.	[112]
Commercial biochar	FeSO <sub>4</sub> and FeCl <sub>3</sub>	Post	Pyrolysis: 500 °C. Magnetization: chemical precipitation and wet impregnation.	Modification decreased adsorption	35 mg/g	<ul style="list-style-type: none"> <li>Ion exchange</li> <li>Precipitation</li> </ul>	This study showed a decrease in adsorption capacity.	[89]
Pinewood	MnCl <sub>2</sub> ·4H <sub>2</sub> O and birnessite (KMnO <sub>4</sub> precipitate)	Pre and post	Pyrolysis in the presence of MnCl <sub>2</sub> ·4H <sub>2</sub> O (MPB): 600 °C for 1 h. Impregnated with birnessite via precipitation following pyrolysis (BPB).	2–20 times	17 mg/g	<ul style="list-style-type: none"> <li>Physical sorption on sites provided by birnessite</li> <li>Precipitation</li> </ul>	The modification process using MnCl <sub>2</sub> resulted in an increase in the surface area and pore volume, potentially due to the formation of Mn-bearing minerals.	[113]
Silkworm excrement	Chitosan combined with pyromellitic dianhydride (GBC)	Post	<ul style="list-style-type: none"> <li>Pyrolysis: 600 °C for 2 h → BC.</li> <li>Chitosan-BC: wet impregnation.</li> <li>Chitosan-BC-PD: wet impregnation (GBC).</li> </ul>	12%	9.54 mg/g	<ul style="list-style-type: none"> <li>Surface complexation</li> <li>Ion exchange</li> <li>Electrostatic interaction</li> </ul>	Modification increased the surface area pore volume, and OFG content.	[114]
Hickory wood	NaOH	Post/during	Wet impregnation, followed by pyrolysis at 600 °C for 2 h.	4.7 times	19.1 mg/g	<ul style="list-style-type: none"> <li>Physical adsorption</li> <li>Surface complexation</li> </ul>	Modification promoted more adsorption sites and increased OFGs.	[58]
Rice straw	KMnO <sub>4</sub>	Post	Wet impregnation.	2.5 times	304.5 mg/g	<ul style="list-style-type: none"> <li>Surface complexation</li> </ul>	Modification increased OFGs, surface area, and pore volume.	[99]
Hickory wood	KMnO <sub>4</sub>	Pre	Wet impregnation.	3.5 times	153.1 mg/g	<ul style="list-style-type: none"> <li>Surface complexation</li> </ul>	Modification provided more binding sites and introduced more OFGs.	[115]

Table 2. Cont.

Feedstock	Modifying Agent/Compound	Pre-Pyrolysis/ Post-Pyrolysis	Production Method	Sorption Increase	Maximum Adsorption	Removal Mechanism/Kinetic Model/Isotherm Model	Key Findings/Notes	Reference
Hickory wood and sugarcane bagasse	Carbon nanotubes (CNT) with the aid of a surfactant	Pre	Pyrolysis: 600 °C for 1 h and wet impregnation of surfactant and CNT.	25–28%	15 mg/g	<ul style="list-style-type: none"> <li>• Surface complexation</li> <li>• Electrostatic interaction</li> </ul>	Sodium dodecylbenzenesulfonate (SDBS), the surfactant, played a crucial role in preventing the aggregation of CNTs and promoting their distribution and stabilization on the BC surface. This resulted in the provision of binding sites for Pb(II) adsorption through CNT nanoparticle interactions.	[116]
<ul style="list-style-type: none"> <li>• Bamboo</li> <li>• Sugarcane bagasse</li> <li>• Hickory wood</li> <li>• Peanut hull</li> </ul>	Chitosan	Post	Feedstock was first converted to biochar by pyrolysis—600 °C for 2 h. Prepared biochar was then modified by chitosan.	5 times	71.5 mg/g	<ul style="list-style-type: none"> <li>• Surface complexation</li> </ul>	Chitosan enhanced the adsorption process by providing binding sites.	[106]
Corn cob	MgCl <sub>2</sub>	Pre	450 °C for 1 h	9.34 times	526.20 mg/g	<ul style="list-style-type: none"> <li>• Precipitation</li> <li>• Complexation</li> <li>• Ion exchange</li> </ul>	Modification increased the crystalline CaCO <sub>3</sub> and OFGs, as well as the surface area and pore volume.	[100]
Peanut shell	MnSO <sub>4</sub> and KHCO <sub>3</sub>	Pre and post	Pyrolysis: 600 °C for 1 h. Wet impregnation.		225 mg/g	<ul style="list-style-type: none"> <li>• Physical adsorption</li> <li>• Freundlich isotherm</li> <li>• Intraparticle diffusion</li> </ul>	Although MnO is used to provide additional adsorption advantages, its micropores can sometimes hinder the diffusion of heavy metals within them. To overcome this limitation, KHCO <sub>3</sub> was added to increase the pore channel of biochar. This facilitated the adsorption of Pb(II) by the formation of a new composite, HMO-K-BC.	[104]

Biochar-based composites can be produced by impregnation or coating by metal oxides, clay minerals, carbonaceous structures (graphene oxide or carbon nanotubes), complex organics, or by inoculation with micro-organisms where biochar can act as a scaffold for embedding new materials [90,99,100,102,117–119]. Wu et al. conducted their modification study using coconut shell as a feedstock and  $\text{MgCl}_2$  as a modifying agent [55]. Modification increased the pore volume to some extent but not significantly enough to demonstrate physical adsorption as the dominant mechanism. The modified biochar was more capable of exchanging Mg for Pb(II) compared to the unmodified biochar, which resulted in a 49-time increase in the ion exchange capacity. In addition to naturally present minerals, impregnation with  $\text{MgCl}_2$  resulted in the generation of MgO and  $\text{Mg}(\text{OH})\text{Cl}$  after pyrolysis, which increased the extent of mineral precipitation. Modification increased the intensity of the aromatic C=C unit, and after the adsorption of Pb(II), there was a decrease in the aromatic C=C intensity. It is well established that cyclic aromatic functional groups serve as donors of  $\pi$  electrons during the adsorption process [120]. Therefore, alterations in these groups are indicative of their involvement in the adsorption mechanism. This study also investigated the adsorption of Pb(II) in the presence of other metals and found that the sorption of Pb(II) was unaffected by the presence of other metals (K, Na, and  $\text{Ca}^{2+}$ ), except for Cd, which showed a significant decrease in sorption when Pb(II) was present. This observation was attributed, by with the researchers, with the fact that Pb(II) is a hard Lewis acid, resulting in a greater affinity for hydroxyl and carboxyl groups present on the biochar surface (which act as hard Lewis bases) towards Pb(II) compared to Cd or other metals [55]. Wang et al. modified biochar using hydrous manganese oxide and found that an optimum impregnation of 3.65% of Mn yielded an increased Pb(II) adsorption [115]. Figure 5 demonstrates the average sorption increase, in terms of percentage, achieved by different modification methods, with metal salts being the highest contributor.

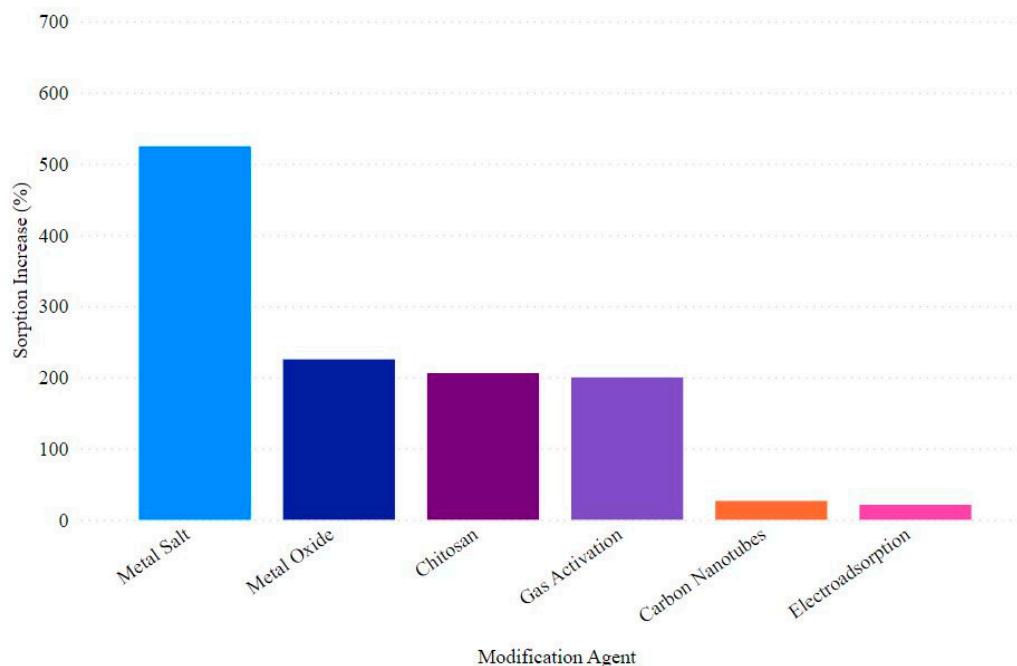


**Figure 5.** Sorption increase (%) by modification agent.

Liu et al. [105] conducted a modification study by  $\text{CO}_2$  activation. Their intention was to increase the carbon and ash component (in form of carbonate and phosphate) of biochar to improve Pb(II) removal through mineral precipitation. Cassava Root Husk-derived biochar was combined with ZnO nanoparticles, which increased the adsorption by up to 28% [107]. The adsorption model followed both PFO and PSO, which indicates that chemisorption also occurred by interactions among the involved components, such as

ion exchange and surface precipitation [64]. However, modification did not significantly increase the surface area and porous structure; therefore, physical adsorption was not significant [107]. In this study, modification increased the number of -OH, which appeared to be dropped after adsorption, indicating that precipitation took part in Pb(II) removal. Tho et al. [107] also found that modification increased the -CO group, which was evident in an FTIR spectrum that took part in surface complexation [55]. Mohan et al. conducted a study of magnetizing biochar by the ferrous and ferric salt impregnation of oak wood and oak bark, followed by a NaOH treatment [109], and showed that the distribution of the magnetic iron oxide particles on the surface of biochar has an impact on the accessibility of aqueous Pb(II) ions to the active sites and pores present on the char. This, in turn, affects the number of sites that are available for the adsorption of Pb(II). Therefore, both the kinetic and equilibrium behavior of the adsorption process are influenced by the extent of dispersion of magnetic particles on the biochar surface. Several other researchers [103,107,114,116,119] have investigated the comparative adsorption capacity between magnetic biosorbents and nanoparticle modifications and found that nanoparticles are less favorable for adsorption compared to magnetic biosorbents. This is partly due to the fact that magnetization causes a decrease in pHZPC, which reduces the difference between the pH and pHZPC. This difference in decrease is particularly favorable for the adsorption of heavy metals [92]. Mahdi et al. conducted a study where they used date seed biochar (DSB) as a cathode, copper wire as an anode, a Pb(II) solution as a cell electrolyte, and a DC power supply to employ 0.1 V for 1 h [111]. They observed an initial rapid adsorption, which was attributed to the fast external mass on the highly porous DSB due to the abundance of vacant surface sites. The electric current applied during the DSB-electro process was believed to be responsible for the observed increase in pore structure. This was thought to be due to the repulsion of negatively charged impurities, which in turn led to the opening of pores. Soares et al. investigated Pb(II) removal by modifying sugarcane straw using FeCl<sub>3</sub> [102]. The authors noted that the modification process resulted in an increase in the surface area and an exposure of functional groups due to the deposition of Fe and Cl. However, they did not elaborate on the specific mechanism behind this outcome. The authors suggested that the modification process could have led to the oxidation of Fe<sup>2+</sup> to FeCl<sub>3</sub>, which may have supplied free electrons to the system. These electrons could have potentially contributed to the generation of a negative charge on the biochar surface, leading to enhanced adsorption. However, further research is needed to confirm this hypothesis and better understand the underlying mechanism. Han et al. [89] conducted a study where they modified commercial biochar by magnetite impregnation using FeSO<sub>4</sub> and FeCl<sub>3</sub> and found that although the magnetization process increased the surface area and pore volume of the biochar, the adsorption for Pb(II) reduced from 50 mg/g to 29 mg/g. A reduction in the pH (1.5) during the magnetization process appeared to dissolve the calcite present on the biochar surface, creating pore spaces as well as increasing the pore volume. However, this reduction in adsorption, despite the increase in the surface area and pore volume, indicated that Pb(II) sorption is more related to the OFGs than the surface area [89].

A study was conducted by Bian et al. where they used silkworm excrement as the feedstock, which was pyrolyzed at 600 °C for 2 h and was followed by wet impregnation using chitosan combined with pyromellitic dianhydride [114]. Chitosan is a polymer with amino and hydroxyl groups that can be used to functionalize the surface of biochar and enhance its adsorption properties. When combined with Pyromellitic Dianhydride (PD), the resulting synergistic compound contains functional groups, such as -CONH<sub>2</sub>-, and carboxyl groups that can interact with heavy metals through mechanisms like ion exchange, electrostatic attraction, and surface complexation [114]. While these compounds were used to modify the silkworm excrement, the resulting biochar showed an increased surface area and pore volume and increased OFG content. The synergistic effect of chitosan and PD creates N-C=O, which is responsible for the removal of Pb through complexation. Modification increased the functional groups but decreased the mineral components, so the role of ion exchange and the precipitation mechanism in Pb removal were not significant;

therefore, complexation played a dominant role. This counterbalancing effect is the reason adsorption did not significantly increase after modification [114].

#### 4. Regeneration/Desorption Study

Various researchers [121–124] have conducted studies on the desorption of Pb(II) from biochar to assess its potential for regeneration, which is critical for cost effectiveness and for ensuring the sustainability of biochar as a solution for Pb(II) removal. Another important reason for conducting desorption studies is to investigate the potential hazard of Pb(II) leaching from biochar, if not disposed of in a manner that aligns with sound environmental practices.

Once the biochar reaches full saturation with metal contaminants, desorption can be achieved through the use of desorbents, such as NaNO<sub>3</sub>, HNO<sub>3</sub>, or KNO<sub>3</sub> solutions, at varying concentrations. By providing a substantial quantity of cations, these compounds can effectively substitute the Pb(II) bonded on the biochar and facilitate the regeneration of the adsorbent [90].

Trakal et al. investigated the desorption of Pb(II) from a magnetically modified nut shell, wheat straw, grape stalk, and husk biochar using NaNO<sub>3</sub>, CaCl<sub>2</sub>, and HNO<sub>3</sub> [103]. They found that after magnetically modifying the biochar, the desorption of Pb(II) was reduced for all chemicals. However, this also demonstrated that the main sorption mechanism was ion exchange and not precipitation. Wu et al. conducted a regeneration experiment of MgCl<sub>2</sub>-modified biochar using NaOH as an eluent [55]. These researchers then conducted five consecutive cycles of adsorption and desorption using the regenerated biochar and found a 25% reduction in the adsorption capacity. This reduction in adsorption is likely attributed to the precipitation caused by the elution, which leads to the blockage of the pores, hindering the adsorption process. Wang et al. investigated the regeneration of biochar from the residue of a magnetic eucalyptus leaf using EDTA-2Na [123] and found a ~21% reduction in the adsorption capacity after the first cycle. Pan et al. explored the regeneration of nitrogen-phosphorous-modified biochar, which demonstrated only a slight decrease in adsorption, even after the 4th cycle. This can be attributed to the deactivation of the functional groups and the blockage of pores, which hinders the sorption process [110]. Mahdi et al. regenerated biochar by reversing the external electric field, and no significant desorption was observed [111]. Sun et al. found about a 50–60% reduction in the adsorption capacity after the 3rd cycle, which can be attributed to structural degradation and the loss of surface minerals [79]. Ding et al. [95] were able to achieve 85% of Pb(II) recovery using HCl. Bian et al. demonstrated only a 7.28% reduction in the adsorption capacity of the silkworm excrement biochar, even after the 5th cycle when NaOH was used as an eluent [114]. Ding et al. investigated the regeneration of hickory wood biochar using HCl [58]. The reduction in adsorption was only 6%, which can be attributed to the other metals not being leached and, therefore, not creating space for adsorption sites for Pb(II). The desorption of Pb(II) from biochar is a critical factor in assessing the potential for its regeneration and sustainability as a solution for Pb(II) removal. Various studies [115,117,125] have investigated the use of different desorbents, such as NaNO<sub>3</sub>, HNO<sub>3</sub>, KNO<sub>3</sub>, CaCl<sub>2</sub>, NaOH solutions, at varying concentrations and found that the effectiveness of desorption and regeneration varies depending on the type of biochar, desorbent, and regeneration method used. Some studies [96,121,124] have shown a reduction in the adsorption capacity after multiple cycles of regeneration due to precipitation, the deactivation of functional groups, and structural degradation. Nevertheless, some studies have demonstrated the successful regeneration of biochar with minimal reduction in the adsorption capacity, such as the use of HCl as a desorbent. Overall, further research is needed to identify optimal methods for the regeneration of biochar and to ensure its sustainable use for Pb(II) removal.

#### 5. Limitation of Studies and Future Scope of Work for Using Biochar as an Adsorbent

The use of biochar for the removal of Pb(II) presents several engineering challenges and opportunities for future research. To date, limited studies [126,127] have investigated

the potential disposal options for Pb(II)-loaded biochar if it is not regenerated, highlighting the need for a comprehensive analysis of toxic Pb(II) leaching from the biochar to identify the most viable management solution for spent biochar. Furthermore, only a few number of studies [43,48,69,101] have explored the column adsorption behavior of biochar that is shown in Figure 6.

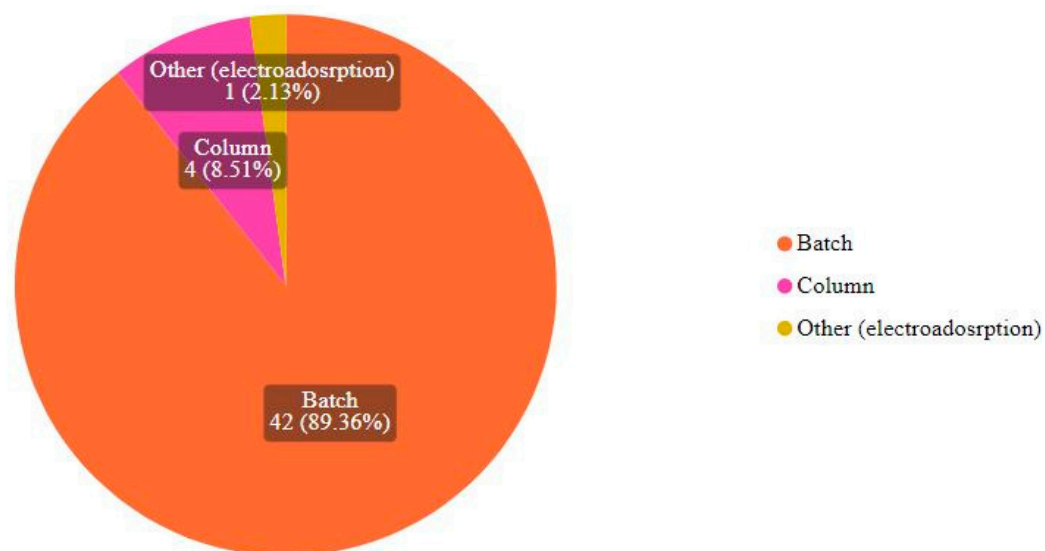


**Figure 6.** Experimental methods adopted by Pb(II) adsorption studies.

The lack of studies conducted on column flow setups presents a critical knowledge gap that must be addressed to advance the technology. More specifically, a thorough understanding of the mechanisms underlying Pb(II) sorption behavior is required to establish design criteria for scaling up the system. It is important to note that the majority of studies [49,66,70,128] to date have focused on monometal solutions, where only one metal is required to be removed. However, in real-world applications, water and wastewater contain a variety of components and contaminants that can significantly affect the Pb(II) sorption behavior of biochar. Thus, a more realistic approach that considers the presence of these compounds is necessary to advance the technology [129]. Biochar is a fluffy low bulk density powder. Batch studies can use this powder directly; however, engineering challenges are encountered when it is to be designed for a column study [67,68]. For a real application, column design is preferred. The packing of fluffy biochar does not seem to be a feasible solution as it may get compacted with time, which would reduce porosity and increase pressure drops across the column. Additionally, if it is not granulated, the chances of biochar leaching out with flow is real. Therefore, there is a need for studying an engineered column set up and bringing an innovative solution such that it becomes a viable alternative of activated carbon for adsorption applications [130].

## 6. Conclusions and Recommendations

In conclusion, this review paper has summarized the last decade of research (2012–2022) on the use of biochar as a metal adsorbent, with a specific focus on Pb. The objective of this review was to provide a comprehensive resource that can guide future researchers in this field. This paper discussed the pyrolysis conditions that can alter the properties of feedstock and convert them to a sorbent called biochar. The physical and chemical properties that play a significant role in the adsorption mechanism were also explored in detail. Additionally, different modification methods were reviewed, with a focus on functionalizing biochar for the specific or enhanced removal of Pb(II).

While the potential of biochar as a metal adsorbent has been widely recognized, this review also highlighted the gaps and limitations in the current literature. For example, limited studies have investigated the potential disposal options for Pb(II)-loaded biochar

and the regeneration of biochar, and there is a lack of studies conducted on column flow setups. Furthermore, the majority of studies have focused on monometal solutions, which may not reflect the complexities of real-world applications.

Moving forward, future research should address these limitations and knowledge gaps by conducting a comprehensive analysis of toxic Pb(II) leaching from the biochar to identify the most viable management solution for spent biochar. Moreover, more studies are needed to establish design criteria for scaling up the system, including a thorough understanding of the mechanisms underlying Pb(II) sorption behavior. Overall, this review highlights the opportunities and engineering challenges associated with using biochar as a metal adsorbent and provides a valuable resource for researchers in this field.

**Author Contributions:** Conceptualization, P.K. and S.K.; methodology, P.K.; software, P.K.; validation, P.K.; formal analysis, P.K.; investigation, P.K.; resources, S.K.; data curation, P.K.; writing—original draft preparation, P.K.; writing—review and editing, P.K. and S.K.; visualization, P.K.; supervision, S.K.; project administration, S.K.; funding acquisition, not applicable. All authors have read and agreed to the published version of the manuscript.

**Funding:** This research received no external funding.

**Conflicts of Interest:** The authors declare no conflict of interest.

## References

1. Lehmann, J.; Joseph, S. *Biochar for Environmental Management: Science, Technology and Implementation*; Routledge: Oxfordshire, UK, 2015. [CrossRef]
2. Hornung, A.; Stenzel, F.; Grunwald, J. Biochar—Just a Black Matter Is Not Enough. *Biomass Convers. Biorefinery* **2021**, 1–12. [CrossRef]
3. Woolf, D.; Lehmann, J.; Cowie, A.; Cayuela, M.L.; Whitman, T.; Sohi, S. Biochar for Climate Change Mitigation: Navigating from Science to Evidence-Based Policy. *Nat. Geosci.* **2018**, 219–248. [CrossRef]
4. Tomczyk, A.; Sokołowska, Z.; Boguta, P. Biochar physicochemical properties: Pyrolysis temperature and feedstock kind effects. *Rev. Environ. Sci. Biotechnol.* **2020**, 19, 191–215. [CrossRef]
5. Kambo, H.S.; Dutta, A. A comparative review of biochar and hydrochar in terms of production, physico-chemical properties and applications. *Renew. Sustain. Energy Rev.* **2015**, 45, 359–378. [CrossRef]
6. Jahirul, M.I.; Rasul, M.G.; Chowdhury, A.A.; Ashwath, N. Biofuels Production through Biomass Pyrolysis—A Technological Review. *Energies* **2012**, 5, 4952–5001. [CrossRef]
7. Mishra, R.K.; Misra, M.; Mohanty, A.K. Value-Added Bio-carbon Production through the Slow Pyrolysis of Waste Bio-oil: Fundamental Studies on Their Structure-Property-Processing Co-relation. *ACS Omega* **2022**, 7, 1612–1627. [CrossRef] [PubMed]
8. Cheah, S.; Jablonski, W.S.; Olstad, J.L.; Carpenter, D.L.; Barthelmy, K.D.; Robichaud, D.J.; Andrews, J.C.; Black, S.K.; Oddo, M.D.; Westover, T.L. Effects of thermal pretreatment and catalyst on biomass gasification efficiency and syngas composition. *Green Chem.* **2016**, 18, 6291–6304. [CrossRef]
9. Yaashikaa, P.R.; Kumar, P.S.; Varjani, S.; Saravanan, A. A critical review on the biochar production techniques, characterization, stability and applications for circular bioeconomy. *Biotechnol. Rep.* **2020**, 28, e00570. [CrossRef] [PubMed]
10. Ahmad, M.; Rajapaksha, A.U.; Lim, J.E.; Zhang, M.; Bolan, N.; Mohan, D.; Vithanage, M.; Lee, S.S.; Kim, K.-H. Biochar as a sorbent for contaminant management in soil and water: A review. *Chemosphere* **2014**, 99, 19–33. [CrossRef] [PubMed]
11. Song, W.; Guo, M. Quality variations of poultry litter biochar generated at different pyrolysis temperatures. *J. Anal. Appl. Pyrolysis* **2012**, 94, 138–145. [CrossRef]
12. Basic Principles of Biochar Production. Available online: <https://biochar.international/guides/> (accessed on 17 February 2024).
13. Cárdenas-Aguiar, E.; Gascó, G.; Paz-Ferreiro, J.; Méndez, A. The effect of biochar and compost from urban organic waste on plant biomass and properties of an artificially copper polluted soil. *Int. Biodeterior. Biodegrad.* **2017**, 124, 223–232. [CrossRef]
14. Rafiq, M.K.; Bachmann, R.T.; Rafiq, M.T.; Shang, Z.; Joseph, S.; Long, R. Influence of Pyrolysis Temperature on Physico-Chemical Properties of Corn Stover (*Zea mays* L.) Biochar and Feasibility for Carbon Capture and Energy Balance. *PLoS ONE* **2016**, 11, e0156894. [CrossRef]
15. Li, X.; Shen, Q.; Zhang, D.; Mei, X.; Ran, W.; Xu, Y.; Yu, G. Functional Groups Determine Biochar Properties (pH and EC) as Studied by Two-Dimensional <sup>13</sup>C NMR Correlation Spectroscopy. *PLoS ONE* **2013**, 8, e65949. [CrossRef]
16. Ippolito, J.A.; Laird, D.A.; Busscher, W.J. Environmental benefits of biochar. *J. Environ. Qual.* **2012**, 41, 967–972. [CrossRef] [PubMed]
17. Panwar, N.L.; Pawar, A.; Salvi, B.L. Comprehensive review on production and utilization of biochar. *SN Appl. Sci.* **2019**, 1, 1–19. [CrossRef]

18. Wang, C.; Wang, X.; Li, N.; Tao, J.; Yan, B.; Cui, X.; Chen, G. Adsorption of Lead from Aqueous Solution by Biochar: A Review. *Clean Technol.* **2022**, *4*, 629–652. [CrossRef]
19. Zhang, C.; Shan, B.; Tang, W.; Zhu, Y. Comparison of cadmium and lead sorption by *Phyllostachys pubescens* biochar produced under a low-oxygen pyrolysis atmosphere. *Bioresour. Technol.* **2017**, *238*, 352–360. [CrossRef]
20. Qiu, M.; Liu, L.; Ling, Q.; Cai, Y.; Yu, S.; Wang, S.; Fu, D.; Hu, B.; Wang, X. Biochar for the removal of contaminants from soil and water: A review. *Biochar* **2022**, *4*, 19. [CrossRef]
21. Inyang, M.; Gao, B.; Yao, Y.; Xue, Y.; Zimmerman, A.R.; Mosa, A.; Pullammanappallil, P.; Kim, K.-H.; Ok, Y.S.; Cao, X. A review of biochar as a low-cost adsorbent for aqueous heavy metal removal. *Crit. Rev. Environ. Sci. Technol.* **2016**, *46*, 406–433. [CrossRef]
22. Park, J.H.; Ok, Y.S.; Kim, S.H.; Cho, J.S.; Heo, J.S.; Delaune, R.D.; Seo, D.C. Competitive adsorption of heavy metals onto sesame straw biochar in aqueous solutions. *Chemosphere* **2016**, *142*, 77–83. [CrossRef]
23. Shi, T.; Jia, S.; Chen, Y.; Wen, Y.; Du, C.; Du, C.; Guo, H.; Wang, Z. Adsorption of Pb(II), Cr(III), Cu(II), Cd(II) and Ni(II) onto a vanadium mine tailing from aqueous solution. *J. Hazard. Mater.* **2009**, *169*, 838–846. [CrossRef] [PubMed]
24. Scott, H.L.; Ponsonby, D.; Atkinson, C.J. Biochar: An improver of nutrient and soil water availability-what is the evidence? *Cab Rev. Perspect. Agric. Vet. Sci. Nutr. Nat. Resour.* **2014**, *9*, 1–19. [CrossRef]
25. Jindo, K.; Mizumoto, H.; Sawada, Y.; Sánchez-Monedero, M.Á.; Sonoki, T. Physical and chemical characterization of biochars derived from different agricultural residues. *Biogeosciences* **2014**, *11*, 6613–6621. [CrossRef]
26. Lehmann, J.; Joseph, S. *Biochar for Environmental Management: Science and Technology*; Routledge: London, UK, 2009; pp. 321–332. [CrossRef]
27. Lu, T.; Yuan, H.; Wang, Y.; Huang, H.; Chen, Y. Characteristic of heavy metals in biochar derived from sewage sludge. *J. Mater. Cycles Waste Manag.* **2016**, *18*, 725–733. [CrossRef]
28. Singh, B.P.; Hatton, B.J.; Singh, B.; Cowie, A.L.; Kathuria, A. Influence of biochars on nitrous oxide emission and nitrogen leaching from two contrasting soils. *J. Environ. Qual.* **2010**, *39*, 1224–1235. [CrossRef]
29. Xu, X.; Cao, X.; Zhao, L. Comparison of rice husk- and dairy manure-derived biochars for simultaneously removing heavy metals from aqueous solutions: Role of mineral components in biochars. *Chemosphere* **2013**, *92*, 955–961. [CrossRef]
30. Collin, M.S.; Venkatraman, S.K.; Vijayakumar, N.; Kanimozhi, V.; Arbaaz, S.M.; Stacey, R.S.; Anusha, J.; Choudhary, R.; Lvov, V.; Tovar, G.I.; et al. Bioaccumulation of lead (Pb) and its effects on human: A review. *J. Hazard. Mater. Adv.* **2022**, *7*, 100094. [CrossRef]
31. Rabin, R. The lead industry and lead water pipes “A Modest Campaign”. *Am. J. Public Health* **2008**, *98*, 1584–1592. [CrossRef]
32. Wani, L.; Ara, A.; Usmani, J.A. Lead toxicity: A review. *Interdiscip. Toxicol.* **2015**, *8*, 55–64. [CrossRef] [PubMed]
33. States with the Most Lead Pipes | Best States | U.S. News. Available online: <https://www.usnews.com/news/best-states/articles/states-with-the-most-lead-pipes> (accessed on 30 July 2023).
34. U.S. Environmental Protection Agency. Basic Information about Lead in Drinking Water. Available online: <https://www.epa.gov/ground-water-and-drinking-water/basic-information-about-lead-drinking-water> (accessed on 30 July 2023).
35. How Can Lead Get into My Drinking Water? | US EPA. Available online: <https://www.epa.gov/lead/how-can-lead-get-my-drinking-water> (accessed on 30 July 2023).
36. Health Effects of Lead Exposure. 2022. Available online: <https://www.cdc.gov/nceh/lead/prevention/health-effects.htm> (accessed on 10 February 2024).
37. Markowitz, M.; Knollmann-Ritschel, B.E.C. Educational Case: Lead Poisoning. *Acad. Pathol.* **2017**, *4*, 2374289517700160. [CrossRef]
38. Learn about Lead | US EPA. Available online: <https://www.epa.gov/lead/learn-about-lead> (accessed on 30 July 2023).
39. Navas-Acien, A.; Guallar, E.; Silbergeld, E.K.; Rothenberg, S.J. Lead exposure and cardiovascular disease—A systematic review. *Environ. Health Perspect.* **2007**, *115*, 472–482. [CrossRef]
40. Florea, A.M.; Taban, J.; Varghese, E.; Alost, B.T.; Moreno, S.; Büsselberg, D. Lead (Pb<sup>2+</sup>) neurotoxicity: Ion-mimicry with calcium (Ca<sup>2+</sup>) impairs synaptic transmission. A review with animated illustrations of the pre- and post-synaptic effects of lead. *J. Local Glob. Health Sci.* **2013**, *2013*, 4. [CrossRef]
41. *Biden-Harris Administration Announces New Get the Lead Out Initiative*; USEPA: Washington, DC, USA, 2023.
42. WHO. Lead in Drinking-Water. 2003. Available online: <https://iris.who.int/handle/10665/75370> (accessed on 11 February 2024).
43. Komkiene, J.; Baltreinaite, E. Biochar as adsorbent for removal of heavy metal ions [Cadmium(II), Copper(II), Lead(II), Zinc(II)] from aqueous phase. *Int. J. Environ. Sci. Technol.* **2016**, *13*, 471–482. [CrossRef]
44. Qu, J.; Zhang, B.; Tong, H.; Liu, Y.; Wang, S.; Wei, S.; Wang, L.; Wang, Y.; Zhang, Y. High-efficiency decontamination of Pb(II) and tetracycline in contaminated water using ball-milled magnetic bone derived biochar. *J. Clean. Prod.* **2023**, *385*, 135683. [CrossRef]
45. Zhao, R.; Wang, B.; Wu, P.; Feng, Q.; Chen, M.; Zhang, X.; Wang, S. Calcium alginate-nZVI-biochar for removal of Pb/Zn/Cd in water: Insights into governing mechanisms and performance. *Sci. Total Environ.* **2023**, *894*, 164810. [CrossRef]
46. Ahmed, W.; Mehmood, S.; Mahmood, M.; Ali, S.; Shakoob, A.; Núñez-Delgado, A.; Asghar, R.M.; Zhao, H.; Liu, W.; Li, W. Adsorption of Pb(II) from wastewater using a red mud modified rice-straw biochar: Influencing factors and reusability. *Environ. Pollut.* **2023**, *326*, 121405. [CrossRef]
47. Omid, A.H.; Cheraghi, M.; Lorestani, B.; Sobhanardakani, S.; Jafari, A. Biochar obtained from cinnamon and cannabis as effective adsorbents for removal of lead ions from water. *Environ. Sci. Pollut. Res.* **2019**, *26*, 27905–27914. [CrossRef] [PubMed]

48. Saravanakumar, K.; Sathyamoorthy, M.; Prasad, D.M.; Senthilkumar, R.; Prasad, B.S. Prasad Continuous removal of cadmium and lead ions by biochar derived from date seeds in a packed column reactor. *Desalination Water Treat.* **2022**, *250*, 126–135. [[CrossRef](#)]
49. Ho, S.H.; Yang, Z.K.; Nagarajan, D.; Chang, J.S.; Ren, N.Q. High-efficiency removal of lead from wastewater by biochar derived from anaerobic digestion sludge. *Bioresour. Technol.* **2017**, *246*, 142–149. [[CrossRef](#)]
50. Inyang, M.; Gao, B.; Yao, Y.; Xue, Y.; Zimmerman, A.R.; Pullammanappallil, P.; Cao, X. Removal of heavy metals from aqueous solution by biochars derived from anaerobically digested biomass. *Bioresour. Technol.* **2012**, *110*, 50–56. [[CrossRef](#)] [[PubMed](#)]
51. Mousavi, H.Z.; Hosseynifar, A.; Jahed, V.; Dehghani, S.A.M. Removal of lead from aqueous solution using waste tire rubber ash as an adsorbent. *Braz. J. Chem. Eng.* **2010**, *27*, 79–87. [[CrossRef](#)]
52. Mohan, D.; Singh, P.; Sarswat, A.; Steele, P.H.; Pittman, C.U. Lead sorptive removal using magnetic and nonmagnetic fast pyrolysis energy cane biochars. *J. Colloid Interface Sci.* **2015**, *448*, 238–250. [[CrossRef](#)] [[PubMed](#)]
53. Uchimiya, M.; Lima, I.M.; Klasson, K.T.; Chang, S.; Wartelle, L.H.; Rodgers, J.E. Immobilization of Heavy Metal Ions (CuII, CdII, NiII, and PbII) by Broiler Litter-Derived Biochars in Water and Soil. *J. Agric. Food Chem.* **2010**, *58*, 5538–5544. [[CrossRef](#)] [[PubMed](#)]
54. Wang, Z.; Liu, G.; Zheng, H.; Li, F.; Ngo, H.H.; Guo, W.; Liu, C.; Chen, L.; Xing, B. Investigating the mechanisms of biochar's removal of lead from solution. *Bioresour. Technol.* **2015**, *177*, 308–317. [[CrossRef](#)] [[PubMed](#)]
55. Wu, J.; Wang, T.; Wang, J.; Zhang, Y.; Pan, W.P. A novel modified method for the efficient removal of Pb and Cd from wastewater by biochar: Enhanced the ion exchange and precipitation capacity. *Sci. Total Environ.* **2020**, *754*, 142150. [[CrossRef](#)] [[PubMed](#)]
56. Mu, R.M.; Wang, M.X.; Bu, Q.W.; Liu, D.; Zhao, Y.L. Adsorption of Pb(II) from aqueous solutions by wheat straw biochar. *IOP Conf. Ser. Earth Environ.* **2018**, *191*, 012041. [[CrossRef](#)]
57. Aslam, Z.; Khalid, M.; Naveed, M.; Shahid, M.A.; Aon, M. Evaluation of Green Waste and Popular Twigs Biochar Produced at Low and High Pyrolytic Temperature for Efficient Removal of Metals from Water. *Water. Air. Soil Pollut.* **2017**, *228*, 432. [[CrossRef](#)]
58. Ding, Z.; Ok, Y.S.; Hu, X.; Wan, Y.; Wang, S.; Gao, B. Removal of lead, copper, cadmium, zinc, and nickel from aqueous solutions by alkali-modified biochar: Batch and column tests. *J. Ind. Eng. Chem.* **2016**, *33*, 239–245. [[CrossRef](#)]
59. Xue, Y.; Gao, B.; Yao, Y.; Inyang, M.; Zhang, M.; Zimmerman, A.R.; Ro, K.S. Hydrogen peroxide modification enhances the ability of biochar (hydrochar) produced from hydrothermal carbonization of peanut hull to remove aqueous heavy metals: Batch and column tests. *Chem. Eng. J.* **2012**, *200*, 673–680. [[CrossRef](#)]
60. Saleh, T.A. Surface Science of Adsorbents and Nanoadsorbents. In *Interface Science and Technology*; Academic Press: Cambridge, MA, USA, 2022. [[CrossRef](#)]
61. Largitte, L.; Pasquier, R.J. Pasquier A review of the kinetics adsorption models and their application to the adsorption of lead by an activated carbon. *Chem. Eng. Res. Des.* **2016**, *109*, 495–504. [[CrossRef](#)]
62. Granados, P.; Mireles, S.; Pereira, E.; Cheng, C.-L.; Kang, J. Effects of Biochar Production Methods and Biomass Types on Lead Removal from Aqueous Solution. *Appl. Sci.* **2022**, *12*, 5040. [[CrossRef](#)]
63. Lagergren, S. About the theory of so-called adsorption of soluble substances. *K. Sven. Vetenskapsakademiens Handl.* **1898**, *24*, 1–39.
64. Ho, Y.S.; McKay, G. A Comparison of Chemisorption Kinetic Models Applied to Pollutant Removal on Various Sorbents. *Process Saf. Environ. Prot.* **1998**, *76*, 332–340. [[CrossRef](#)]
65. Kajjumba, G.W.; Emik, S.; Öngen, A.; Özcan, H.K.; Aydın, S. Modelling of Adsorption Kinetic Processes—Errors, Theory and Application. In *Advanced Sorption Process Applications*; IntechOpen: London, UK, 2018. [[CrossRef](#)]
66. Kołodziejka, D.; Wnierzak, R.; Leahy, J.J.; Hayes, M.H.B.; Kwapinski, W.; Hubicki, Z. Kinetic and adsorptive characterization of biochar in metal ions removal. *Chem. Eng. J.* **2012**, *197*, 295–305. [[CrossRef](#)]
67. Gwenzi, W.; Chaukura, N.; Noubactep, C.; Mukome, F.N. Mukome Biochar-based water treatment systems as a potential low-cost and sustainable technology for clean water provision. *J. Environ. Manag.* **2017**, *197*, 732–749. [[CrossRef](#)]
68. Rosales, E.; Mejjide, J.; Pazos, M.; Sanromán, M.Á. Challenges and recent advances in biochar as low-cost biosorbent: From batch assays to continuous-flow systems. *Bioresour. Technol.* **2017**, *246*, 176–192. [[CrossRef](#)] [[PubMed](#)]
69. Boni, M.R.; Chiavola, A.; Marzeddu, S. Remediation of Lead-Contaminated Water by Virgin Coniferous Wood Biochar Adsorbent: Batch and Column Application. *Water. Air. Soil Pollut.* **2020**, *231*, 1–16. [[CrossRef](#)]
70. Chen, X.; Zhu, X.; Fan, G.; Wang, X.; Li, H.; Li, H.; Xu, X. Enhanced adsorption of Pb(II) by phosphorus-modified chicken manure and Chinese medicine residue co-pyrolysis biochar. *Microsc. Res. Tech.* **2022**, *85*, 3589–3599. [[CrossRef](#)]
71. Yılmaz, C.; Güzel, F. Performance of wild plants-derived biochar in the remediation of water contaminated with lead: Sorption optimization, kinetics, equilibrium, thermodynamics and reusability studies. *Int. J. Phytoremediation* **2021**, *24*, 177–186. [[CrossRef](#)]
72. Cui, L.; Yan, J.; Li, L.; Quan, G.; Ding, C.; Chen, T.; Yin, C.; Gao, J.; Hussain, Q. Does Biochar Alter the Speciation of Cd and Pb in Aqueous Solution. *Bioresources* **2014**, *10*, 88–104. [[CrossRef](#)]
73. Kalam, S.; Abu-Khamsin, S.A.; Mahmoud, M.; Kamal, M.S.; Patil, S. Surfactant Adsorption Isotherms: A Review. *ACS Omega* **2021**, *6*, 32342–32348. [[CrossRef](#)]
74. Fahmi, A.H.; Jol, H.; Singh, D. Physical modification of biochar to expose the inner pores and their functional groups to enhance lead adsorption. *RSC Adv.* **2018**, *8*, 38270–38280. [[CrossRef](#)]
75. Chatterjee, A.; Abraham, J. Desorption of heavy metals from metal loaded sorbents and e-wastes: A review. *Biotechnol. Lett.* **2019**, *41*, 319–333. [[CrossRef](#)] [[PubMed](#)]
76. Mukherjee, A.; Patra, B.R.; Podder, J.; Dalai, A.K. Dalai Synthesis of Biochar From Lignocellulosic Biomass for Diverse Industrial Applications and Energy Harvesting: Effects of Pyrolysis Conditions on the Physicochemical Properties of Biochar. *Front. Mater.* **2022**, *9*, 870184. [[CrossRef](#)]

77. Mohan, D.; Pittman, C.U., Jr.; Bricka, M.; Smith, F.; Yancey, B.; Mohammad, J.; Steele, P.H.; Alexandre-Franco, M.F.; Gómez-Serrano, V.; Gong, H. Sorption of arsenic, cadmium, and lead by chars produced from fast pyrolysis of wood and bark during bio-oil production. *J. Colloid Interface Sci.* **2007**, *310*, 57–73. [[CrossRef](#)] [[PubMed](#)]
78. Conz, R.F.; Abbruzzini, T.F.; Andrade, C.D.; Milori, D.M.; Cerri, C.E. Effect of Pyrolysis Temperature and Feedstock Type on Agricultural Properties and Stability of Biochars. *Agric. Sci.* **2017**, *8*, 914–933. [[CrossRef](#)]
79. Sun, C.; Chen, T.; Huang, Q.; Wang, J.; Wang, J.; Wang, J.; Lu, S.; Yan, J. Enhanced adsorption for Pb(II) and Cd(II) of magnetic rice husk biochar by KMnO<sub>4</sub> modification. *Environ. Sci. Pollut. Res.* **2019**, *26*, 8902–8913. [[CrossRef](#)]
80. Major, J.; Steiner, C.; Downie, A.; Lehmann, J. Biochar Effects on Nutrient Leaching. In *Biochar for Environmental Management*; Routledge: London, UK, 2012; pp. 303–320.
81. Muoghalu, C.C.; Owusu, P.A.; Lebu, S.; Nakagiri, A.; Semiyaga, S.; Iorhemen, O.T.; Manga, M. Biochar as a novel technology for treatment of onsite domestic wastewater: A critical review. *Front. Environ. Sci.* **2023**, *11*, 1095920. [[CrossRef](#)]
82. Jin, J.; Li, Y.; Zhang, J.; Wu, S.; Cao, Y.; Liang, P.; Zhang, J.; Wong, M.H.; Wang, M.; Shan, S.; et al. Influence of pyrolysis temperature on properties and environmental safety of heavy metals in biochars derived from municipal sewage sludge. *J. Hazard. Mater.* **2016**, *320*, 417–426. [[CrossRef](#)]
83. Li, H.; Dong, X.; da Silva, E.B.; de Oliveira, L.M.; Chen, Y.; Ma, L.Q. Mechanisms of metal sorption by biochars: Biochar characteristics and modifications. *Chemosphere* **2017**, *178*, 466–478. [[CrossRef](#)]
84. Cao, X.; Ma, L.; Liang, Y.; Gao, B.; Harris, W. Simultaneous Immobilization of Lead and Atrazine in Contaminated Soils Using Dairy-Manure Biochar. *Environ. Sci. Technol.* **2011**, *45*, 4884–4889. [[CrossRef](#)]
85. Zhao, Q.; Wang, Y.; Xu, Z.; Yu, Z.; Yu, Z. Removal mechanisms of Cd(II) and Pb(II) from aqueous solutions using straw biochar: Batch study, Raman and X-ray photoelectron spectroscopy techniques. *Desalination Water Treat.* **2021**, *220*, 199–210. [[CrossRef](#)]
86. Napitupulu, M.; Walanda, D.K.; Simatupang, M. Utilization of red fruit's peel (*freycinetia arborea gaudich*) as biochar for lead (Pb) adsorption. *J. Phys. Conf. Ser.* **2020**, *1434*, 012033. [[CrossRef](#)]
87. Jin, Q.; Wang, Z.; Feng, Y.; Kim, Y.T.; Stewart, A.C.; O'Keefe, S.F.; Neilson, A.P.; He, Z.; Huang, H. Grape pomace and its secondary waste management: Biochar production for a broad range of lead (Pb) removal from water. *Environ. Res.* **2020**, *186*, 109442. [[CrossRef](#)] [[PubMed](#)]
88. Keiluweit, M.; Kleber, M. Molecular-Level Interactions in Soils and Sediments: The Role of Aromatic  $\pi$ -Systems. *Environ. Sci. Technol.* **2009**, *43*, 3421–3429. [[CrossRef](#)] [[PubMed](#)]
89. Han, Z.; Sani, B.; Mroczek, W.; Obst, M.; Beckingham, B.; Karapanagioti, H.K.; Werner, D. Magnetite Impregnation Effects on the Sorbent Properties of Activated Carbons and Biochars. *Water Res.* **2015**, *70*, 394–403. [[CrossRef](#)]
90. Ahmed, M.B.; Zhou, J.L.; Ngo, H.H.; Guo, W.; Chen, M. Progress in the preparation and application of modified biochar for improved contaminant removal from water and wastewater. *Bioresour. Technol.* **2016**, *214*, 836–851. [[CrossRef](#)]
91. Cao, X.; Harris, W.G. Properties of dairy-manure-derived biochar pertinent to its potential use in remediation. *Bioresour. Technol.* **2010**, *101*, 5222–5228. [[CrossRef](#)]
92. Hassan, M.; Naidu, R.; Du, J.; Liu, Q.; Liu, Y.; Liu, Y.P.; Qi, F. Critical review of magnetic biosorbents: Their preparation, application, and regeneration for wastewater treatment. *Sci. Total Environ.* **2020**, *702*, 134893. [[CrossRef](#)]
93. Sayyadian, K.; Moezzi, A.; Gholami, A.; Panahpour, E.; Mohsenifar, K. Ohsenifar Effect of Biochar on Cadmium, Nickel and Lead Uptake and Translocation in Maize Irrigated with Heavy Metal Contaminated Water. *Appl. Ecol. Environ. Res.* **2019**, *17*, 969–982. [[CrossRef](#)]
94. Duku, M.H.; Gu, S.; Hagan, E.B. Biochar production potential in Ghana—A review. *Renew. Sustain. Energy Rev.* **2011**, *15*, 3539–3551. [[CrossRef](#)]
95. Ding, W.; Dong, X.; Ime, I.M.; Gao, B.; Ma, L.Q. Pyrolytic temperatures impact lead sorption mechanisms by bagasse biochars. *Chemosphere* **2014**, *105*, 68–74. [[CrossRef](#)]
96. Lu, H.; Zhang, W.; Yang, Y.; Huang, X.; Wang, S.; Qiu, R. Relative distribution of Pb<sup>2+</sup> sorption mechanisms by sludge-derived biochar. *Water Res.* **2012**, *46*, 854–862. [[CrossRef](#)]
97. Wang, M.C.; Sheng, G.D.; Qiu, Y.P. A novel manganese-oxide/biochar composite for efficient removal of lead(II) from aqueous solutions. *Int. J. Environ. Sci. Technol.* **2015**, *12*, 1719–1726. [[CrossRef](#)]
98. Liang, J.; Li, X.; Yu, Z.; Zeng, G.; Luo, Y.; Jiang, L.; Yang, Z.; Qian, Y.; Wu, H. Amorphous MnO<sub>2</sub> Modified Biochar Derived from Aerobically Composted Swine Manure for Adsorption of Pb(II) and Cd(II). *ACS Sustain. Chem. Eng.* **2017**, *5*, 5049–5058. [[CrossRef](#)]
99. Tan, G.; Wu, Y.; Liu, Y.; Xiao, D. Removal of Pb(II) ions from aqueous solution by manganese oxide coated rice straw biochar A low-cost and highly effective sorbent. *J. Taiwan Inst. Chem. Eng.* **2018**, *84*, 85–92. [[CrossRef](#)]
100. Deng, Y.; Li, X.; Ni, F.; Liu, Q.; Yang, Y.; Wang, M.; Ao, T.; Chen, W. Synthesis of Magnesium Modified Biochar for Removing Copper, Lead and Cadmium in Single and Binary Systems from Aqueous Solutions: Adsorption Mechanism. *Water* **2021**, *13*, 599. [[CrossRef](#)]
101. Huang, K.; Cai, Y.; Du, Y.; Song, J.; Mao, H.; Xiao, Y.; Wang, Y.; Yang, N.; Wang, H.; Han, L. Adsorption of Pb(II) in Aqueous Solution by the Modified Biochar Derived from Corn Straw with Magnesium Chloride. *Nat. Environ. Pollut. Technol.* **2020**, *19*, 1273–1278. [[CrossRef](#)]

102. Soares, M.B.; dos Santos, F.H.; Alleoni, L.R. Iron-Modified Biochar from Sugarcane Straw to Remove Arsenic and Lead from Contaminated Water. *Water, Air, Soil Pollut.* **2021**, *232*, 1–13. [[CrossRef](#)]
103. Trakal, L.; Veselská, V.; Šafařík, I.; Vítková, M.; Čihalová, S.; Komárek, M. Lead and cadmium sorption mechanisms on magnetically modified biochars. *Bioresour. Technol.* **2016**, *203*, 318–324. [[CrossRef](#)] [[PubMed](#)]
104. Wan, S.; Qiu, L.; Tang, G.; Weiyang, C.; Li, Y.; Gao, B.; He, F. Ultrafast sequestration of cadmium and lead from water by manganese oxide supported on a macro-mesoporous biochar. *Chem. Eng. J.* **2020**, *387*, 124095. [[CrossRef](#)]
105. Liu, Y.; Zhu, X.; Wei, X.; Zhang, S.; Jie, J.; Chen, J.; Ren, Z.J. CO<sub>2</sub> Activation Promotes Available Carbonate and Phosphorus of Antibiotic Mycelial Fermentation Residue-Derived Biochar Support for Increased Lead Immobilization. *Chem. Eng. J.* **2018**, *334*, 1101–1107. [[CrossRef](#)]
106. Zhou, Y.; Gao, B.; Zimmerman, A.R.; Fang, J.; Sun, Y.; Cao, X. Sorption of heavy metals on chitosan-modified biochars and its biological effects. *Chem. Eng. J.* **2013**, *231*, 512–518. [[CrossRef](#)]
107. Tho, P.T.; Van, H.T.; Nguyen, L.H.; Hoang, T.K.; Tran, T.N.; Nguyen, T.T.; Nguyen, T.B.; Le Sy, H.; Tran, Q.B.; Sadeghzadeh, S.M.; et al. Enhanced simultaneous adsorption of As(III), Cd(II), Pb(II) and Cr(VI) ions from aqueous solution using cassava root husk-derived biochar loaded with ZnO nanoparticles. *RSC Adv.* **2021**, *11*, 18881–18897. [[CrossRef](#)] [[PubMed](#)]
108. Liu, S.; Zhang, S.; Fan, M.; Yuan, Y.; Sun, X.; Wang, D.; Xu, Y. High-efficiency adsorption of various heavy metals by tea residue biochar loaded with nanoscale zero-valent iron. *Environ. Prog.* **2021**, *40*, e13706. [[CrossRef](#)]
109. Mohan, D.; Kumar, H.; Sarswat, A.; Alexandre-Franco, M.; Pittman, C.U., Jr. Cadmium and lead remediation using magnetic oak wood and oak bark fast pyrolysis bio-chars. *Chem. Eng. J.* **2014**, *236*, 513–528. [[CrossRef](#)]
110. Pan, J.; Deng, H.; Du, Z.; Tian, K.; Zhang, J. Design of nitrogen-phosphorus-doped biochar and its lead adsorption performance. *Environ. Sci. Pollut. Res.* **2022**, *29*, 28984–28994. [[CrossRef](#)]
111. Mahdi, Z.; Hanandeh, A.E.; Yu, Q.; Yu, Q.J. Electro-assisted adsorption of heavy metals from aqueous solutions by biochar. *Water Sci. Technol.* **2020**, *81*, 801–812. [[CrossRef](#)]
112. Jellali, S.; Diamantopoulos, E.; Haddad, K.; Anane, M.; Durner, W.; Mlayah, A. Lead removal from aqueous solutions by raw sawdust and magnesium pretreated biochar: Experimental investigations and numerical modelling. *J. Environ. Manag.* **2016**, *180*, 439–449. [[CrossRef](#)]
113. Wang, S.; Gao, B.; Li, Y.; Mosa, A.; Zimmerman, A.R.; Ma, L.Q.; Harris, W.G.; Migliaccio, K.W. Manganese oxide-modified biochars: Preparation, characterization, and sorption of arsenate and lead. *Bioresour. Technol.* **2015**, *181*, 13–17. [[CrossRef](#)]
114. Bian, P.; Liu, Y.; Zheng, X.; Shen, W. Removal and Mechanism of Cadmium, Lead and Copper in Water by Functional Modification of Silkworm Excrement Biochar. *Polymers* **2022**, *14*, 2889. [[CrossRef](#)]
115. Wang, H.; Gao, B.; Wang, S.; Fang, J.; Xue, Y.; Yang, K.; Yang, K. Removal of Pb(II), Cu(II), and Cd(II) from aqueous solutions by biochar derived from KMnO<sub>4</sub> treated hickory wood. *Bioresour. Technol.* **2015**, *197*, 356–362. [[CrossRef](#)] [[PubMed](#)]
116. Inyang, M.; Gao, B.; Zimmerman, A.R.; Zhou, Y.; Cao, X. Sorption and cosorption of lead and sulfapyridine on carbon nanotube-modified biochars. *Environ. Sci. Pollut. Res.* **2015**, *22*, 1868–1876. [[CrossRef](#)] [[PubMed](#)]
117. Gupta, S.; Sireesha, S.; Sreedhar, I.; Patel, C.M.; Anitha, K.L. Latest trends in heavy metal removal from wastewater by biochar based sorbents. *J. Water Process Eng.* **2020**, *38*, 101561. [[CrossRef](#)]
118. Rajapaksha, A.U.; Chen, S.S.; Kim, K.-H.; Tsang, D.C.W.; Zhang, M.; Zhang, M.; Vithanage, M.; Mandal, S.; Gao, B.; Bolan, N.; et al. Engineered/designer biochar for contaminant removal/immobilization from soil and water: Potential and implication of biochar modification. *Chemosphere* **2016**, *148*, 276–291. [[CrossRef](#)]
119. Sizmur, T.; Fresno, T.; Akgül, G.; Frost, H.; Moreno-Jiménez, E. Biochar modification to enhance sorption of inorganics from water. *Bioresour. Technol.* **2017**, *246*, 34–47. [[CrossRef](#)] [[PubMed](#)]
120. Cui, X.; Siyu, F.; Yiqiang, Y.; Vogt, R.D.; Li, T.; Ni, Q.; Wang, C.-H.; Yang, X.; He, Z. Potential mechanisms of cadmium removal from aqueous solution by *Canna indica* derived biochar. *Sci. Total Environ.* **2016**, *562*, 517–525. [[CrossRef](#)] [[PubMed](#)]
121. Lata, S.; Singh, P.K.; Samadder, S.R. Regeneration of adsorbents and recovery of heavy metals: A review. *Int. J. Environ. Sci. Technol.* **2015**, *12*, 1461–1478. [[CrossRef](#)]
122. Odega, C.A.; Ayodele, O.O.; Ogotuga, S.O.; Anguruwa, G.T.; Adekunle, A.E.; Fakorede, C.O. Potential Application and Regeneration of Bamboo Biochar for Wastewater Treatment: A Review. *Adv. Bamboo Sci.* **2022**, *2*, 100012. [[CrossRef](#)]
123. Wang, S.Y.; Tang, Y.K.; Chen, C.; Wu, J.T.; Huang, Z.; Mo, Y.Y.; Zhang, K.X.; Chen, J.B. Regeneration of magnetic biochar derived from eucalyptus leaf residue for lead(II) removal. *Bioresour. Technol.* **2015**, *186*, 360–364. [[CrossRef](#)]
124. Alsawy, T.; Rashad, E.; El-Qelish, M.; Mohammed, R.H. A comprehensive review on the chemical regeneration of biochar adsorbent for sustainable wastewater treatment. *Npj Clean Water* **2022**, *5*, 29. [[CrossRef](#)]
125. Wang, B.; Gao, B.; Fang, J. Recent advances in engineered biochar productions and applications. *Crit. Rev. Environ. Sci. Technol.* **2017**, *47*, 2158–2207. [[CrossRef](#)]
126. Zhao, J. Valorization and reuse of waste modified biomass. In *Heavy Metal Biosorption Removal from Aqueous Solutions*; Universitat Autònoma de Barcelona: Bellaterra, Spain, 2019.
127. Zhang, W.; Huang, X.; Jia, Y.; Rees, F.; Tsang, D.C.; Qiu, R.; Wang, H. Metal immobilization by sludge-derived biochar: Roles of mineral oxides and carbonized organic compartment. *Environ. Geochem. Health* **2017**, *39*, 379–389. [[CrossRef](#)]

128. Tripathi, M.; Sahu, J.N.; Ganesan, P.B. Effect of process parameters on production of biochar from biomass waste through pyrolysis: A review. *Renew. Sustain. Energy Rev.* **2016**, *55*, 467–481. [[CrossRef](#)]
129. Uday, V.; Harikrishnan, P.S.; Deoli, K.; Zitouni, F.; Mahlkecht, J.; Kumar, M. Current Trends in Production, Morphology, and Real-World Environmental Applications of Biochar for the Promotion of Sustainability. *Bioresour. Technol.* **2022**, *359*, 127467. [[CrossRef](#)]
130. Oliveira, F.R.; Patel, A.K.; Jin, Y.; Jaisi, D.P.; Adhikari, S.; Lu, H.; Khanal, S.K. Environmental application of biochar: Current status and perspectives. *Bioresour. Technol.* **2017**, *246*, 110–122. [[CrossRef](#)]

**Disclaimer/Publisher's Note:** The statements, opinions and data contained in all publications are solely those of the individual author(s) and contributor(s) and not of MDPI and/or the editor(s). MDPI and/or the editor(s) disclaim responsibility for any injury to people or property resulting from any ideas, methods, instructions or products referred to in the content.